Distribution Agreement

In presenting this thesis as a partial fulfillment of the requirements for a degree from Emory University, I hereby grant to Emory University and its agents the non-exclusive license to archive, make accessible, and display my thesis in whole or in part in all forms of media, now or hereafter now, including display on the World Wide Web. I understand that I may select some access restrictions as part of the online submission of this thesis. I retain all ownership rights to the copyright of the thesis. I also retain the right to use in future works (such as articles or books) all or part of this thesis.

Erdong Chen April 15th, 2015

Localization of $Ca_v3.1$ T-Type calcium channels in the thalamus of normal and parkinsonian monkeys: light and electron microscopic immunocytochemistry using subtype-specific antibodies

by

Erdong Chen

Dr. Yoland Smith, Ph.D.
Adviser

Emory University Department of Biology

Dr. Yoland Smith, Ph.D.

Adviser

Dr. Dieter Jaeger, Ph.D.

Committee Member

Dr. Samuel Sober, Ph.D.

Committee Member

April 15th, 2015

Localization of $Ca_v3.1$ T-Type calcium channels in the thalamus of normal and parkinsonian monkeys: light and electron microscopic immunocytochemistry using subtype-specific antibodies

by

Erdong Chen

Dr. Yoland Smith, Ph.D.

Adviser

An abstract of
a thesis submitted to the Faculty of Emory College of Arts and Sciences
of Emory University in partial fulfillment
of the requirements of the degree of
Bachelor of Sciences with Honors

Emory University Department of Biology

April 15th, 2015

Abstract

Localization of $Ca_v3.1$ T-Type calcium channels in the thalamus of normal and parkinsonian monkeys: light and electron microscopic immunocytochemistry using subtype-specific antibodies

By Erdong Chen

The motor dysfunction of Parkinson's disease results from degeneration of the nigrostriatal dopaminergic system, and the consequent functional changes of basal ganglia-thalamocortical circuits. Changes in thalamic activity, including an increase in burst discharges of thalamic neurons, are associated with the development of parkinsonism. In part, the abnormal bursting activity in PD may involve de-inactivation of T-type calcium channels (Ca_v3) following neuronal hyperpolarization. It is unclear whether this abnormal thalamic burst activity is the result of altered hyperpolarization from basal ganglia inputs, or changes in T-type calcium channel localization and function. To address the involvement of T-type calcium channels in abnormal thalamic activity, we studied the cellular, subcellular, and subsynaptic localization of the $Ca_v3.1$ channel in the ventrolateral (VL) and centromedian/parafascicular (CM/Pf) thalamic nuclei, the main thalamic targets of basal ganglia outflow, in normal and parkinsonian monkeys. At the light microscopic level, strong $Ca_v3.1$ neuropil immunoreactivity was found throughout the thalamus. The intensity of immunolabeling in CM/Pf was lower than in VL. There was no significant difference in the overall pattern and intensity of immunostaining between normal and parkinsonian monkeys. At the electron microscopic level, most $Ca_v3.1$ immunoreactivity was found in dendritic shafts of various sizes, with 40-60% and 30-40% dendritic profiles displaying $Ca_v3.1$ immunoreactivity in the VL and CM/Pf, respectively. At the subcellular level, aggregates of $Ca_v3.1$ immunoperoxidase and immunogold labeling were commonly found in the post-synaptic densities of putative asymmetric glutamatergic synapses and putative symmetric GABAergic synapses, suggesting potential roles in both excitatory and inhibitory neurotransmission. The pattern of subcellular and subsynaptic localization of $Ca_v3.1$ between normal and parkinsonian monkeys was not significantly different. Thus, any involvement of T-type calcium channels in increased thalamic bursting firing activities in the parkinsonian state is likely mediated by altered hyperpolarization of thalamic neurons rather than changes in channel expression.

Localization of $Ca_v3.1$ T-Type calcium channels in the thalamus of normal and parkinsonian monkeys: light and electron microscopic immunocytochemistry using subtype-specific antibodies

By

Erdong Chen

Dr. Yoland Smith, Ph.D.

Adviser

A thesis submitted to the Faculty of Emory College of Arts and Sciences
of Emory University in partial fulfillment
of the requirements of the degree of
Bachelor of Sciences with Honors

Emory University Department of Biology

April 15th, 2015

Table of Contents

I. Introduction

Background: Parkinson's disease (PD) in humans is a neurodegenerative disorder that develops with the progressive death of midbrain dopaminergic neurons, depletion of dopamine in areas of the brain that receive dopaminergic inputs from those neurons, and intracytoplasmic Lewy body accumulation. The term "Parkinsonism" refers to a spectrum of physical motor abnormalities that occur post-dopaminergic neurodegeneration. Clinically, PD is characterized by motor symptoms such as rest tremor, postural instability, stiffness and rigidity of the limbs and trunk, shuffling gait, decreased ambulatory arm swing, hypokinesia (decreased movement), bradykinesia (slowness in movement execution), and akinesia (inability to initiate movement). Additionally, those afflicted by PD can also experience non-motor symptoms such as diminished or loss of sense of smell, sleep disorders, cognitive impairment, and depression (Miller and DeLong, 1988). The manifestation of these symptoms significantly decrease quality of life for many patients.

Pathophysiology of Parkinsonism: The exact mechanisms responsible for the development of parkinsonism have yet to be elucidated. However, it is widely accepted that loss of dopamine in the nigrostriatal dopaminergic pathway which links the substantia nigra pars compacta (SNc) with the striatum plays an essential role in the genesis of parkinsonian motor complications (Parent and Hazrati, 1995; Smith and Villalba, 2008). Traditionally, the "rate model" of the basal ganglia suggests that outputs are mostly inhibitory (GABAergic) and dopamine release from nigrostriatal projection neuron terminals modulate thalamocortical activity via a direct (monosynaptic) and indirect (polysynaptic) pathway (Galvan and Wichmann, 2008). The internal segment of the globus pallidus (GPi) and the substantia nigra pars reticulata (SNr) tonically function in the inhibition of their target nuclei in the thalamus and the brainstem. In healthy

humans, striatal dopamine release and activation of the direct pathway via dopamine binding to D_1 receptors facilitates transmission from the striatum to the internal pallidum. The tonically active neurons found in the internal pallidum are briefly suppressed. This decrease in tonic basal ganglia inhibitory output allows for increased activity of thalamocortical projection neurons (Wichmann and DeLong, 1996; DeLong and Wichmann, 2007). In the indirect pathway, dopamine binding to D_2 receptors acts to inhibit thalamocortical transmission (Gerfen, 1995; DeLong and Kandel, 2013) (Fig, 1). In parkinsonism, it is estimated that substantial neuronal degeneration of around 70% in the nigrostriatal dopaminergic tract must occur for motor symptoms to become significant (Bernheimer et al., 1973). The degeneration of these neurons ultimately results in alterations in direct and indirect pathways and increased excitatory input from the subthalamic nucleus (STN) to the internal globus pallidus (GPi) and substantia nigra pars reticulata (SNr). The consequent increased inhibition of the ventral anterior and ventrolateral (VA/VL) and the intralaminar centromedian and parafascicular (CM/Pf) nuclei of the thalamus is thought to underlie hypokinetic dysfunction and parkinsonian motor symptoms. In support of the increased activity of the GPi and SNr in PD pathology proposed by the rate model, ablative lesioning of these the STN and GPi in both the 1-methyl-4-phenyl-1,2,3,6-tetrahydropyridine (MPTP)-treated primate model of parkinsonism and human PD patients yield symptomatic improvement (Bergman et al., 1990; Aziz et al., 1991; Lozano et al., 1995; Baron et al., 1996; Alvarez et al., 2005; Galvan and Wichmann, 2008).

Current treatments, challenges, and research motivations: Beginning with the discovery of Levodopa and the efficacy of dopamine replacement therapy in the 1960s (Hornykiewicz, 2010), there have been tremendous advances in the treatment of dopamine-deficiency parkinsonism. In the 1990s, the advent of deep brain stimulation (DBS) of the subthalamic nucleus (STN) and the

GPi led to further clinically significant improvement in quality of life for those afflicted with PD (Bergman et al., 1994; Limousin et al., 1995). Though the effectiveness of these therapies are incontrovertible, they require diligence in monitoring both by the patient and the physician and are often associated with significant adverse side effects, particularly in patients who have been on dopamine replacement therapy for 5-10 years following a diagnosis (Marsden, 1994). Additionally, these therapies have not been shown to beneficially affect the underlying pathology of the disease. Though the understanding of the pathophysiology of PD in humans has increased significantly over the last half-century, efforts by researchers to slow down, halt, or even reverse the highly ordered process of programmed cell death (PCD) that is responsible for the dopaminergic neurodegeneration seen in PD have yet to yield clinically substantial benefits. Anti-apoptotic neuroprotective therapies that show great potential in animal studies have consistently failed to produce the same effects in human clinical trials (Olanow et al., 2008). With this stagnation and the adverse extrapyramidal side effects of long-term Levodopa therapy in patients with advanced PD that include fluctuations, dyskinesias, toxicity, or loss of efficacy (Marsden, 1994), there is an onus for researchers to develop alternative or complementary therapies that can be used to replace or supplement existing approaches. This critical need has prompted the research detailed in this manuscript. Here, we report on a study of the localization of T-type calcium channels (Ca_v3) in the thalamus of normal and MPTP-treated parkinsonian monkeys. These channels mediate abnormal burst firing activity in the pathological state throughout the basal ganglia and thalamus that is thought to underlie some of the motor deficits of the disease. The development of selective compounds that target these channels could potentially yield novel therapies for PD that improve quality of life for many patients.

Basal ganglia-thalamocortical dysrhythmia in parkinsonism: The onset and progression of Parkinsonian symptoms in primates has been closely linked to aberrant function of the basal ganglia-thalamocortical circuits (BGTC) (Bergman et al., 1994; Magnin et al., 2000; Galvan and Wichmann, 2008). The crucial involvement of the STN is underscored by the proven efficacy of procedures such as subthalamotomy and DBS that target the structure in animal models and in patients (Krack et al.; Bergman et al., 1994; Limousin et al., 1995; Guridi et al., 1996; Su et al., 2002; Alvarez et al., 2005; Hamani et al., 2007; Alvarez et al., 2009). However, the exact mechanisms through which these interventions exact their clinical benefit are not concretely understood. It is not currently known why delivery of electrical stimulation by itself can significantly ameliorate a condition that arises from the progressive loss of a biological compound. Even more puzzling perhaps, is the fact that both inhibition of activity through lesioning and electrical stimulation of the STN both yield significant symptomatic improvement in patients with advanced PD. Recent studies proposed therapeutic reduction of aberrant calcium channel mediated electrical activity within the BGTC as a potential explanatory factor for the efficacy of these approaches (Yang et al., 2014).

T-type calcium channels and parkinsonism: Calcium channels in mammalian systems play a variety of critical roles in muscle contraction, regulation of gene expression, initiation of synaptic transmission, integration of synaptic input, and regulation of action potential firing (Catterall, 2011). In cardiac myocytes and neurons of the thalamus, T-type calcium channels (Ca_v3 subfamily; $\alpha1G/Ca_v3.1$, $\alpha1H/Ca_v3.2$, $\alpha1I/Ca_v3.3$) mediate repetitive firing of action potentials in rhythmically active cells. Additionally, these channels play a prominent role in the pathogenesis of various neurological disorders. Abnormal subthalamic or thalamic T-type calcium channel firing activity has been demonstrated in insomnia, absence epilepsy,

neuropathic pain, and PD (Bergman et al., 1994; Destexhe et al., 1994; Kim et al., 2001; Lee et al., 2004; Steriade, 2005; Khosravani and Zamponi, 2006; Nelson et al., 2006; Zhang et al., 2013; Dragicevic et al., 2015). Neurons in the STN and thalamus typically fire in regular or irregular single spikes or in bursts characterized by densely packed groups of spikes in repeats (Fig. 2) (Llinas and Jahnsen, 1982b; Yang et al., 2014). Distinct changes in firing patterns of neurons in the STN, especially an increased tendency for burst discharge, have been reported both in parkinsonian humans and in animal models of parkinsonism (Bergman et al., 1994; Hutchison et al., 1994; Song et al., 2000; Vila et al., 2000). In fact, increased burst firing in the basal ganglia has been accepted as a pathological hallmark of parkinsonism (Bergman et al., 1998). One type of increased burst discharge, termed "rebound bursting" has been described intracellularly (Llinas and Jahnsen, 1982a). Rebound bursting is characterized by low threshold calcium spike bursts (LTS) that result from hyperpolarization induced de-inactivaton of T-type calcium channels, which are normally voltage inactivated at resting membrane potential (Magnin et al., 2000). A LTS, when generated, produces one to several grouped sodium spikes. Certain features of these bursts, including a typical interburst frequency of 3-6 Hz, are synchronous with parkinsonian symptoms such as classical tremor and have been implicated as a causal factors (Pare et al., 1990; Yang et al., 2014).

Current research and study rationale: In the STN of 6-hydroxydopamine—lesioned (6-OHDA lesioned) parkinsonian rats, recent evidence suggests that delivery of negative depolarizing current into the extracellular space decreases the availability of T-type calcium channels. The consequent reduction in rebound bursting is accompanied by improvement of locomotion. Accordingly, the injection of positive current mediated the opposite effect through increased hyperpolarization and de-inactivation of T-type calcium channels (Tai et al., 2012). The

pathological increase in rebound bursts has also been documented in the thalamus of PD patients and animal models of parkinsonism, specifically in nuclei that receive afferents from the basal ganglia. The neurons in these thalamic nuclei are evolutionarily related to and exhibit very similar spike/burst kinetics as neurons in the STN (Marchand, 1987; McCormick and Bal, 1994, 1997; Timmermann et al., 2003). Increased rebound bursting has been documented in the ventrolateral (VL) and ventroanterior (VA) nuclei of the thalamus (Magnin et al., 2000; Pessiglione et al., 2005). Additionally, studies exploring DBS in the posterior intralaminar centromedian and parafascicular (CM/Pf) complex of the thalamus suggest that the targeting of these nuclei may maximize clinical benefit in some subsets of patients by reducing tremor and freezing even more so than targeting of the STN (Mazzone et al., 2006; Peppe et al., 2008). It is conceivable that these findings and reported symptomatic benefits can also be interpreted as a result of a reduction in T-type calcium channel mediated rebound bursting.

Considering the success of DBS and its supposed mechanism of action, pharmacological normalization of T-type calcium channel mediated bursting activity potentially could also serve to alleviate parkinsonian motor symptoms. This hypothesis has been tested in the STN of 6-OHDA lesioned parkinsonian rats using specific channel antagonists (Tai et al., 2011). This study provided evidence that T-type calcium channels are crucial for the genesis of burst discharge, and that T-type calcium channel antagonists not only inhibit LTS activity in the STN, but also alleviate locomotor deficits in parkinsonian rats. Thus, application of T-type calcium channel antagonist drugs in the MPTP-treated primate model of PD may also produce similar results. As part of an ongoing research program to address this issue, we characterized the anatomical substrate through which such drugs could mediate their effects upon thalamic activity. With the availability of isoform-selective anti-$Ca_v3.1$ antibodies, the cellular and

ultrastructural localization of this channel can now be investigated in the thalamus where the a1G subtype of T-type calcium channel is the most widely expressed channel isoform (Talley et al., 1999). Therefore, using light microscopy and electron microscopy immunoperoxidase and immunogold labeling methods with a specific monoclonal $Ca_v3.1$ antibody, we studied the cellular, subcellular, synaptic, and subsynaptic localization of the a1G subtype of T-type calcium channel in the ventrolateral (VL) and centromedian (CM) and parafascicular (Pf) thalamic nuclei, the main thalamic targets of basal ganglia outflow, in rhesus monkeys. Elucidation of differences in the spatial distribution of these channels in normal and parkinsonian monkeys will aid in the optimization of specific channel antagonist compounds that can potentially mediate robust anti-parkinsonian effects and serve as alternatives or complements to current dopamine replacement and surgical intervention therapies.

II. Material and methods

General experimental strategy: We used light and electron microscopy with a subtype specific antibody to study the distribution of the a1G subtype of T-type calcium channel in the basal ganglia-receiving territories of the ventrolateral, centromedian, and parfasicular thalamic nuclei in normal and parkinsonian monkeys.

Animals: Six adult Rhesus monkeys (*Macaca mulatta*, 5-10 kg) were used in this study. The anatomical localization work was conducted using three control and three MPTP-treated monkeys. Pre-mortem, all animals were pair-housed, and had *ad libitum* access to food and water. All experiments were performed in accordance with the United States Public Health Service Policy on the humane care and use of laboratory animals, including the provisions of the

"Guide for the Care and Use of Laboratory Animals" (Garber et al., 2011). All studies were approved by the Biosafety and Animal Care and Use Committee of Emory University.

Three of the animals were treated with MPTP (0.2-0.6mg/kg i.m.; Sigma, St. Louis, MO; cumulative doses: 2.8 - 8.8 mg/kg) once per week, until they reached comparable states of stable moderate parkinsonism. The degree and stability of the MPTP-induced motor disability was assessed as previously described (Devergnas et al., 2014). Briefly, animals were evaluated weekly using an observation cage equipped with infrared beams, allowing us to measure their body movements as infrared beam break events. A parkinsonism rating scale was also used to quantify impairments in ten aspects of motor function (bradykinesia, freezing, extremity posture, trunk posture, action tremor, the frequency of arm and leg movements, finger dexterity, home cage activity, and balance), each scored on a 0 to 3 scale (maximal score 30). For the three MPTP-treated monkeys, the final parkinsonian rating score ranged between 13 to 20, corresponding to moderately severe parkinsonism. The severity of the parkinsonian motor signs had to be stable for a period of at least 6 weeks after the last MPTP injection before the decision was made to sacrifice the animal.

Perfusion of Animals and sectioning of tissue: To terminate the experiment, the animals were sacrificed with an overdose of sodium pentobarbital (100 mg/kg, i.v.) and transcardially perfused with cold oxygenated Ringer's solution, followed by a fixative containing 4% paraformaldehyde and 0.1% glutaraldehyde in a phosphate buffer (PB) solution. After perfusion, the brains were removed from the skull, cut coronally into 10 mm thick blocks, and post-fixed overnight in 4% paraformaldehyde. The blocks were then cut into 60μm-thick coronal sections using a vibrating microtome and stored at -20 ˚C in an anti-freeze solution, containing 30% ethylene glycol and 30% glycerol in PB, until ready for immunohistochemistry.

Immunohistochemistry

Antibodies used: The commercial sources and characteristics of the monoclonal and polyclonal primary antibodies generated against $Ca_v3.1$, and vGluT2 used in this study are detailed in Table 1.

Specificity tests of $Ca_v3.1$ antibody: For the localization of $Ca_v3.1$, we used a highly specific monoclonal antibody (NINDS/NIMH NeuroMab, Davis, CA). According to the supplier, this antibody reacts with the >250kDa molecular weight protein associated with $Ca_v3.1$, does not cross-react with other subtypes of Ca_v3 channels, and does not result in any significant immunostaining or Western blot band labeling in tissue from $Ca_v3.1$ knockout mice (NeuroMab; Accession # Q9WUT2).

To further assess the specificity of this antibody for its use in the present study, a Western blot was performed on fresh monkey brain tissue (generous gift from Dr. Anthony Chan, Ph.D., Yerkes Primate Research Center, Emory University, Atlanta, GA, USA). The frozen tissue was homogenized by sonication in buffer (150 mM NaCl, 10 mM HEPES, 1 mM EGTA, and 0.1 mM MgCl2, pH 7.4, with 0.5% TritonX-100) with complete anti-protease (Cat No. 11245200, Roche, IN, USA), and the protein concentration was determined by Bradford reagent (Bio-Rad, Hercules, CA). The immunoprecipitation was performed with the $Ca_v3.1$ antibody and samples were resolved by SDS-PAGE on a 4-15% gel (Invitrogen, CA, USA). The protein content was analyzed by immunoblotting and immunoreactivity was detected by enhanced chemiluminescence (GE Healthcare, Little Chalfont, Buckinghamshire, UK). This experiment served to confirm antibody specificity and a high level of $Ca_v3.1$ expression in the monkey thalamus (Fig. 3).

Selection of Monkey Brain Tissue: Selection of 60nm thick sections of thalamic tissue containing the VL and CM/Pf thalamic nuclei were chosen as defined in *The Rhesus Monkey Brain in Stereotaxic Coordinates* (Paxinos et al., 1999). Sections chosen for the VL corresponded approximately to IA:11.55 and sections chosen for the CM/Pf corresponded to IA: 7.95 as defined in the stereotaxic atlas.

Light microscopic pre-embedding immunoperoxidase procedures: Sections of tissue to be processed were removed from the anti-freeze solution and then placed in phosphate-buffered saline (PBS, 0.01M, pH 7.4). They were immersed in sodium borohydride (1% in PBS) for 20 minutes and incubated for 1 hour in PBS containing 1% normal horse serum (NHS), 1% bovine serum albumin (BSA), and 0.3% Triton X-100, followed by incubation in the primary antibody (anti-$Ca_v3.1$) solution containing 1% NHS, 1% BSA, and 0.3% Triton X-100 in PBS for 24 hours at 4°C. Sections were then rinsed three times in PBS and subsequently incubated in the secondary antibody solution containing 1% NHS, 1% BSA, 0.3% Triton X-100, and biotinylated horse anti-mouse IgGs (Vector Laboratories, Burlingame, CA; used at 1:200 dilution) for 90 minutes at room temperature. After three rinses in PBS, the sections were incubated for 90 minutes in avidin-biotin peroxidase complex (ABC) solution (Vectastain standard ABC kit, Vector Laboratories; used at 1:100 dilution) including 1% BSA. To reveal the antigenic sites, the sections were first rinsed with PBS and Tris buffer (50 mM; pH 7.6), and then incubated in a solution containing 0.025% 3, 3'-diaminobenzidine tetrahydrochloride (DAB; Sigma), 10 mM imidazole, and 0.005% hydrogen peroxide in Tris buffer for 10 min. The sections were subsequently washed several times in PBS, mounted on gelatin-coated glass slides, dehydrated, and coverslipped with Cytoseal XYL™ (Richard-Allan Scientific). The slides were scanned at 20X using a ScanScope CS scanning light microscope system (Aperio Technologies, Vista, CA). Digital representations of the slides were

saved and analyzed using the ImageScope software (Aperio). To help with the delineation of the nuclear borders between the basal ganglia- and cerebellar-receiving territories of the ventral motor nuclei, some adjacent sections were immunostained for the vesicular glutamate transporter 2 (vGluT2) using highly specific antibodies (Mab Technologies, Atlanta, GA, USA) and immunohistochemical procedures described in detail in our previous studies (Villalba et al., 2006; Raju et al., 2008; Kuramoto et al., 2011). Additional adjacent sections from representative control and MPTP-treated monkeys were immunostained for tyrosine hydroxylase (TH) using immunohistochemical procedures detailed in our previous studies (Mazloom and Smith, 2006; Mathai et al., 2015) in order to demonstrate the substantial reduction in dopamine conferred by MPTP-treatment of the monkeys used in this study.

Electron microscopic pre-embedding immunoperoxidase protocol: Sections were immersed in sodium borohydride (1% in PBS) for 20 minutes, rinsed in PBS, and placed in a cryoprotectant solution (0.05M PB, pH 7.4, 25% sucrose and 10% glycerol) for 20 minutes prior to being frozen at -80°C for 20 minutes and thawed to permeabilize cell membranes. Then, sections were put through a graded series of cryoprotectant solution (100%, 70%, 50%, and 30% in PBS), and finally washed in PBS. The subsequent tissue processing was identical to that used for light microscopy, up to the point of the use of DAB, with two important differences: Triton X-100 was omitted from all solutions, and sections were incubated in the primary antibody solution for 48h at 4°C. After DAB exposure, the tissue was rinsed in PB (0.1 M, pH 7.4) and treated with 1% osmium tetroxide for 20 min. The sections were then dehydrated through an increasing gradient of ethanol (50%, 70%, 90% and 100%) with the initial incubation done in 70% solution containing 1% uranyl acetate for 35 minutes to increase contrast under the EM. The sections were then placed in propylene oxide and subsequently embedded in epoxy resin (Durcupan, ACM; Fluka, Buchs,

Switzerland) for 24 hours. Then, the sections were mounted on microscope slides, dabbed with epoxy resin, coverslipped with mineral oil-coated coverslips, and put in the oven at 60°C for 48 hours to cure the resin. After polymerization, the coverslips were taken off, and small blocks of tissue from the basal ganglia-receiving area of the ventrolateral, centromedian, and parafasicular nuclei were cut from the slides and glued onto resin blocks with cyanoacrylate glue. The blocks were cut into 60nm-thin sections using a diamond knife ultramicrotome (Ultracut T2; Leica, Nussloch, Germany) and collected on single-slot Pioloform-coated copper grids. The sections were then stained with lead citrate for 5 minutes, rinsed in distilled water, and viewed under a transmission electron microscope (JEM-1011; JEOL USA Inc., Peabody, MA).

Electron microscopic pre-embedding immunogold protocol: The tissue was prepared as described above, except that sections were pre-incubated in PBS containing 5% milk, rinsed in Tris Buffer Saline-Gelatin (TBS-Gelatin), and silver-intensified gold particles were coupled to secondary antibodies, as described in our previous studies (Kuwajima et al., 2007; Mitrano et al., 2010; Gonzales et al., 2013).

Densitometric Analysis of Light Microscopy Material: Using Imagescope image viewing software (Aperio), we analyzed digital 0.4x magnification images of immunostained tissue slides containing the motor thalamus in a manner similar to that reported in our previous studies (Galvan et al., 2011). The images were converted into 16-bit grayscale format and inverted. The intensity of $Ca_v3.1$ immunoreactivity was determined by measuring the optical density of $Ca_v3.1$ immunoperoxidase labeling in the GPi-receiving territory of the ventral motor thalamic nuclei of control and MPTP-treated monkeys with ImageJ Software (National Institutes of Health, (Schneider et al., 2012). Adjacent vGluT2-immunostained sections were used to help delineate the thalamic nuclei borders. Three measurements for optical density were taken in adjacent $2.08mm^2$

areas of $Ca_v3.1$ immunostained tissue per animal in the region of interest (ROI). Total area analyzed is summarized in Table 2. Average optical density was calculated per animal in the ROI by taking the mean of the optical density measurements. Additional optical density measurements were taken in the internal capsule immediately adjacent to thalamic boarders in each section in the same manner and averaged to reflect background labeling. The values for background labeling were subtracted from that obtained in the thalamic ROIs. The Mann—Whitney rank sum test was conducted using the background-corrected values to assess statistical significance of differences between measurements made in tissue from control and MPTP-treated monkeys.

Analysis of Electron Microscopy Material: To assess the localization of $Ca_v3.1$ labeling in normal and parkinsonian animals, fifty digital micrographs of randomly encountered $Ca_v3.1$-labeled neuronal elements were captured in each animal at 40,000X magnification and saved with a CCD camera (Orius 78; Gatan, Inc., Pleasanton, CA) that was controlled by DigitalMicrograph software (Gatan Microscopy Suite), yielding 2214 μm^2 of tissue analyzed per nucleus per animal. Additional micrographs of clearly representative immunoreactivity were taken at 100,000X for illustrative purposes and were not included in the analysis. Immunoperoxidase labeling could be identified as a dark, amorphous deposit within neuronal elements, while immunogold labeling appeared as small dark, round particles within neuronal elements.

Immunoperoxidase: Peroxidase-immunoreactive elements were classified based on ultrastructural features (Peters et al., 1991), and the relative distribution of $Ca_v3.1$ immunoreactivity amongst neuronal elements was compared between normal and MPTP-treated animals. Labeled dendrites were categorized into small ($\leq$0.5μM), medium (0.5μM-1μM), or large ($\geq$1μM) profiles, based on their cross-sectional diameter. The same immunoperoxidase-stained sections were used to assess the relative prevalence of $Ca_v3.1$-labeled dendrites over the total population of dendritic profiles

in the VL, CM, and Pf as well as the relative percentage of synaptically associated dendritic labeling over the total population of immunoreactive dendritic profiles. For this classification, amorphous deposits direct attached to postsynaptic specializations were classified as "synaptic" and dendritic immunoreactivity was otherwise deemed "extrasynaptic". Values obtained for all measures were compared between control and MPTP-treated animals using either student's t-test or Welche's t-test, depending on the assumptions of variance of the groups as determined by the F-test.

Immunogold: The immunogold-stained sections were used to elucidate the specific localization of $Ca_v3.1$ labeling at the putative glutamatergic synapses and GABAergic synapses. Glutamatergic and GABAergic synapses were differentiated based the types of postsynaptic contacts they established. Synapses with thick post-synaptic densities were classified as glutamatergic and those with minimal post-synaptic densities were assumed to be GABAergic. Furthermore, the immunoreactivity of gold particles was classified into four categories (extrasynaptic, intracellular, synaptic, and perisynaptic) based on their localization in relation to the plasma membrane and postsynaptic specializations visible in the tissue plane in a fashion similar to that used in previous reports from our laboratory (Kuwajima et al., 2007).The gold particles that were directly on or within 20 nm of the plasma membrane were identified as "plasma membrane-associated", and pooled into three categories (i.e., synaptic, perisynaptic, and extrasynaptic) based on their localization relative to postsynaptic specializations. In this manuscript, the term "synaptic" is used to describe gold particles found within the main body of postsynaptic specializations, whereas "perisynaptic" refers to gold particles found within 20 nm from the edges of postsynaptic specializations. Perisynaptic and synaptic labeling was presumed to be associated with an epitope present at the synapse. All other plasma membrane-bound gold particles were categorized as

"extrasynaptic". The gold particles that were located more than 20 nm away from the plasma membrane were categorized as "intracellular", and presumed to be non-associated with the substrates located on the plasma membrane. The 20-nm cut-off point was chosen based on the assertion that the distance between the immunoreactive substrate and gold particle, bridged by the primary and secondary antibodies, can be approximate to 20 nm (Blackstad et al., 1990). Statistical analyses were performed using the same procedures described for the immunoperoxidase data.

III. Results

Western blot for $Ca_v3.1$ expression in thalamic and striatal tissue: The western blot analysis revealed a high degree of antibody specificity. A single band corresponding to the predicted molecular weight (>250kDa) of $Ca_v3.1$ was observed in both thalamic and striatal tissue, with greater expression in the thalamic tissue compared to the striatal tissue (Fig. 3).

Tyrosine hydroxylase stain reveals dopamine depletion in the basal ganglia following treatment with MPTP: In control monkeys, a high level of TH immunoreactivity corresponding to the degree of enzymatic conversion of L-DOPA to dopamine was observed in the striatum (caudate nucleus [CN] and putamen [Put]) and the SN (Fig. 4 A). As described previously (Kuwajima et al., 2007; Villalba et al., 2009; Mathai et al., 2015), in the MPTP-treated macaque model of parkinsonism, neurotoxicity confers a significant loss of dopamine and consequent TH-immunoreactivity (Fig. 4 B) in the nigrostriatal dopamine system of more than 90%.

Light microscopic immunohistochemical staining for $Ca_v3.1$ in the monkey thalamus: At the LM level, staining for $Ca_v3.1$ revealed a high degree of expression for the α1G subtype of T-type calcium channel in the neuropil of the monkey thalamus (Fig. 5). This is consistent with previous immunohistochemical and electrophysiological reports of channel immunoreactivity and burst

firing in thalamic nuclei (Huguenard et al., 1993; Yunker et al., 2003; McKay et al., 2006; Cain and Snutch, 2013). The intralaminar CM/Pf complex displayed a comparable level of between nuclei immunoreactivity both pre and post-MPTP treatment ($p = 0.39$ control; $p = 0.40$ post-MPTP; t-test) but significantly less staining compared to the VL ($p < 0.001$ control; $p < 0.05$ post-MPTP; t-test) (Fig. 5 E). Though $Ca_v3.1$ mediated burst firing has been reported in numerous studies in the VL, the intralaminar nuclei have received much less attention. At high magnification, immunoreactivity was apparent throughout the neuropil, with clear localization in the perikarya and dendritic processes. Treatment with MPTP did not yield any significant differences in $Ca_v3.1$ labeling density in all three nuclei compared to control animals ($p > 0.05$ VL, CM, and Pf; Mann-Whitney Rank Sum Test). (Fig. 5 E). No labeling was observed in the striatum or the globus pallidus (GP), where burst firing has not been reported. Additional immunostained cerebellar sections of control monkeys revealed $Ca_v3.1$ expression restricted to somatic and dendritic regions of Purkinje cells in the molecular layer (data not shown), consistent with the findings of previous imaging and electrophysiological studies (Cavelier and Bossu, 2003; McKay et al., 2006; Hildebrand et al., 2009; Isope et al., 2012), further substantiating the high specificity of the antibody used.

EM immunoperoxidase localization of $Ca_v3.1$ in the VL and posterior intralaminar CM/Pf:

At the EM level, across all three nuclei and both experimental conditions in this study, the vast majority (~80-90%) of α1G T-type calcium channel immunoreactivity in the monkey thalamus was localized to postsynaptic dendrites of various sizes. Immunoreactivity was also encountered in unmyelinated axons (~3-9%) and rarely in cell bodies, glia, and presynaptic terminals (<4%) (Fig. 6). Overall, the data indicate that MPTP-treatment did not alter the pattern of $Ca_v3.1$ expression in the neuronal elements of the VL, CM, and Pf. The only statistically significant

difference was a reduction in the CM from 3.35% to 1.92% in the percentage of total immunoreactive elements represented by glia ($p = 0.014$; t-test) post MPTP-treatment (Fig. 6 E).

Aggregates of peroxidase within immunoreactive small (≤0.5μM), medium (0.5μM-1μM), and large (≥1μM) dendrites (Fig. 7 A-C) were commonly found in association with the cell membrane and in the post-synaptic specializations of putative asymmetric glutamatergic synapses (Fig. 7 panel D). Additional quantification included the percentage of dendritic profiles expressing $Ca_v3.1$ immunoreactivity out of the total population of dendritic profiles within the area of tissue analyzed (Fig. 7 F-G). Again, MPTP-treatment did not result in statistically significant changes across all nuclei studied ($0.13 < p < 0.88$; t-test). However, the comparison between nuclei confirms the lower level of $Ca_v3.1$ expression in the CM/Pf compared to the VL evident in the densitometric studies. In the neuropil of the CM/Pf, only ~35% of all dendritic profiles demonstrated peroxidase immunoreactivity compared to ~50% in the VL. EM peroxidase also revealed $Ca_v3.1$ expression along the dendritic tree. Quantification of immunoreactive dendrite cross sectional diameter allowed for an understanding of dendritic $Ca_v3.1$ expression relative to the perikaryon. Peroxidase reactivity in large dendrites indicated proximal channel expression while reactivity in small dendrites indicated distal expression. In all nuclei, $Ca_v3.1$ immunoreactivity was found evenly distributed across small and medium dendrites and seldom encountered in large dendritic profiles. In the monkey thalamus, MPTP-treatment did not significantly alter the distribution of $Ca_v3.1$ along the dendritic arbor (Fig. 7 I). These data indicate that $Ca_v3.1$ is expressed all along the length of dendrites in the monkey thalamus. However, care should be taken when interpreting the data as evidence of a predominantly distal expression. The high level of peroxidase reactivity in small and medium dendrites and relatively low level in large dendrites is likely due to the number of each

dendrite size present in the neuropil of the thalamus. Due to dendritic arborization, small and medium sized dendrites intuitively have a much larger presence compared to large dendrites.

EM immunogold localization of $Ca_v3.1$ in the VL and intralaminar CM/Pf: Though immunoperoxidase is a highly sensitive approach for protein localization that benefits from excellent penetrance, dense aggregation of amorphous peroxidase at the epitope makes it unsuitable for study of subcellular and subsynaptic localization. Thus, we used pre-embedding immunogold to further investigate the synaptic localization of $Ca_v3.1$ apparent from the immunoperoxidase studies and potential alterations in T-type calcium channel expression in monkeys treated with MPTP. The overall pattern of immunoreactivity amongst neuronal elements was similar to that found in the immunoperoxidase studies. $Ca_v3.1$ was found to be localized predominantly in dendrites of various size, with additional labeling observed in axons, terminals, glia, and cell bodies. The vast majority (75-87%) of the $Ca_v3.1$ immunogold labeling in dendrites was found in direct association with the plasma membrane (Fig. 8 A-D). MPTP-treatment did not significantly affect relative plasma membrane expression of $Ca_v3.1$ in the VL and Pf. However, the data for the CM indicated a statistically significant post-MPTP increase in relative expression ($p = 0.02$; t-test) (Fig. 8 E). Gold particles were often encountered directly on (synaptic) and within 20nm of the edge (perisynaptic) of putative symmetric GABAergic synapses and putative asymmetric glutamatergic synapses (Fig. 8 A, C, and D). Of the total membrane immunogold labeling for $Ca_v3.1$ in dendrites of both control and MPTP-treated animals, 12-17% of the gold particles were found in association with synapses (aggregated synaptic and perisynaptic classifications) across all three nuclei. Generally, across all three nuclei and both experimental conditions, synaptic and perisynaptic labeling by gold particles was evenly distributed amongst symmetric (~5-9%) and asymmetric synapses (~4-10%) (Fig. 9 A). In the VL, MPTP-treatment

caused a marginally significant increase in the relative percentage of membrane bound labeling found at symmetric synapses compared to control data ($p = 0.043$; t-test, * in Fig. 9 A). However, similar significance was not observed in the CM and Pf. The relative proportion of membrane bound labeling found at asymmetric synapses was not significantly affected by MPTP-treatment in any of the nuclei studied. In between nuclei analysis, a marginally significant difference was found in the number of immunoreactive symmetric synapses per area of tissue in the Pf of control animals ($p = 0.037$, single-factor ANOVA, * in Fig. 9 B). This difference was likely due to the lower number of observed immunoreactive symmetric synapses in the Pf compared to the VL and CM. Between nuclei and treatment groups, there were no significant differences in the number of asymmetric synapses. Finally, MPTP-treatment decreased the ratio of immunoreactive asymmetric to symmetric synapses with marginal significance only in the CM ($p = 0.037$, t-test, * in Fig. 9 C). The ratio of immunoreactive asymmetric to symmetric synapses in the VL and Pf was not significantly affected.

IV. Discussion

The results of this work suggest that the α1G subtype of T-type calcium channel is widely expressed in neurons of the VL, CM, and Pf thalamic nuclei and that MPTP-treatment generally does not significantly alter its cellular and subcellular localization. The main findings are as follows: (1) $Ca_v3.1$ is widely expressed in various neuronal elements of the primate thalamus, predominantly along the dendritic arbor but also to a lesser extent in axons, terminals, glia, and cell bodies, (2) the density of $Ca_v3.1$ expression in the VL is significantly higher than in the posterior intralaminar CM/Pf complex, (3) subcellularly, $Ca_v3.1$ is localized primarily along the cellular membrane of dendrites of various sizes, (4) $Ca_v3.1$ is present along the dendritic membrane post-synaptically in areas that form both symmetric GABAergic synapses and

asymmetric glutamatergic synapses with presynaptic terminals, and (5) in the primate model of parkinsonism utilized in this study, treatment with MPTP and consequent confirmed dopaminergic neurodegeneration generally does not have a profound effect on the density, cellular and subcellular localization, and synaptic and subsynaptic localization of $Ca_v3.1$ T-type calcium channels in the VL, CM, and Pf nuclei of the monkey thalamus. Together, these findings provide strong evidence for a potentially significant role played by thalamic $Ca_v3.1$ T-type calcium channels in normal physiological states and in the genesis of pathological dysrhythmias in PD.

$Ca_v3.1$ is widespread and diverse in its localization throughout the human body. $Ca_v3.1$ T-type channels have been shown to mediate physiological functions primarily in the brain but also in the ovaries, placenta, heart, kidneys, and lungs. Due to their significant expression in the brain and proposed roles in the pathogenesis of a number of neurological disorders, the specific molecular mechanisms of the physiological roles played by T-type calcium channels in neurons has been a much studied topic (Perez-Reyes, 2003). The dendritic channel localization found in this study is consistent with the findings of studies examining the localization of T-type calcium channels in neuronal populations throughout the brain. Studies have demonstrated the preferential localization of $Ca_v3.1$ to dendrites in the hippocampus and cerebellum (Christie et al., 1995; Kavalali et al., 1997; Gauck et al., 2001), as well as basal ganglia nuclei such as the STN (Song et al., 2000). A study investigating the dendritic expression of different channel isoforms in thalamic relay neurons reported that all Ca_v3 channels are expressed in the soma and that $Ca_v3.1$ and $Ca_v3.3$ is present throughout the dendritic arbor and may show preference for distal regions while $Ca_v3.2$ tends to be localized to proximal dendrites (McKay et al., 2006). The

findings of the present study offer support for the assertion that $Ca_v3.1$ is localized predominantly to dendrites and shows preference for distal dendrites.

The difference in intensity of immunoreactivity between the VL and CM/Pf complex found in this study is interesting. At the LM level, there appears to be a wide discrepancy in the degree of peroxidase immunoreactivity between the VL and CM/Pf, with the VL displaying a much darker immunoreactivity profile. However, the EM data show that the difference between VL and CM/Pf in dendritic expression of $Ca_v3.1$ is only ~15%. The cellular and subcellular anatomy as well as the electrophysiological properties of neurons in the posterior intralaminar CM/Pf complex are not well characterized. Though it is well known and accepted that T-type calcium channels mediate robust burst firing activity throughout the thalamus (Llinas and Jahnsen, 1982b), the implications and significance of their differential expression between nuclei are unclear. Since the profile of immunoreactivity along the dendritic arbor is consistent across all three nuclei, an increase in distal expression of $Ca_v3.1$ in the VL compared to the CM/Pf cannot explain this observed phenomenon, It may be possible that neurons in the CM/Pf in fact do express less $Ca_v3.1$ compared to the VL, or that the observed difference in density of labeling could be due to innate differences in anatomy. Differences in neuropil between the VL and CM/Pf, specifically in the distribution and arborization of dendrites (which accounted for the majority of immunoreactivity) represent an area worthy of further investigation and could serve to explain the difference in intensity of immunoreactivity.

The predominant membrane localization of $Ca_v3.1$ can be interpreted as channel insertion in the plasma membrane, and the low level of intracellular immunoreactivity likely represents protein trafficking to the cell surface. At their localization on the membranes of dendrites, $Ca_v3.1$ channels likely mediate low voltage activated calcium spikes. Somatic or dendritic calcium spike

discharge has been documented in various neuronal populations (Kampa et al., 2006) and could potentially contribute to dendritic low voltage activated calcium responses in neurons of the VL, CM, and Pf. The widespread membrane localization of $Ca_v3.1$ along the full length of the dendritic arbor implicate these channels in this activity. The role played by T-type calcium channels in dendritic calcium influx has been previously characterized (Zhou et al., 1997). Increases in intracellular concentrations of calcium may also facilitate its role as a second messenger in a variety of cellular processes such as modulation of enzyme activity and the activity of other channels.

The postsynaptic immunogold labeling observed in association with symmetric and asymmetric synapses suggests a possible role of thalamic $Ca_v3.1$ in inhibitory and excitatory neurotransmission. The dense localization of $Ca_v3.1$ to dendrites and its role in calcium influx in synaptic integration and signal amplification has been documented (Markram and Sakmann, 1994; Destexhe et al., 1998). Markram and Sakmann found in pyramidal cells of the rat neocortex that subthreshold excitatory postsynaptic potentials, elicited by the activation of glutamate receptor channels, caused a brief increase in dendritic Ca^{2+}. This rise in dendritic Ca^{2+} was mediated by the opening of LVA channels in the dendritic membrane (Markram and Sakmann, 1994). In cerebellar Purkinje neurons, recent work has shown that $Ca_v3.1$ physically and functionally couples to metabotropic glutamate receptor 1 (mGluR1). Both the synaptic and pharmacological activation of mGluR1 results in a robust and reversible potentiation of $Ca_v3.1$-mediated T-type transients within Purkinje cells (Isope et al., 2012). Additionally, work coming from the same lab has shown that $Ca_v3.1$ in the cerebellum is localized primarily to dendritic spines. This implicates them in synaptic events (Hildebrand et al., 2009). Though the functional

interactions of thalamic $Ca_v3.1$ with postsynaptic receptors and contributions to synaptic signaling are not well understood, similar functional significance is conceivable.

With increased burst firing activity documented in the BGTC of animal models of parkinsonism and in humans with PD, it seems counterintuitive that in this study, treatment of monkeys with MPTP and subsequent induction of parkinsonism was not accompanied by changes in the cellular and subcellular localization of $Ca_v3.1$ T-type calcium channels in the thalamus. With increased burst firing activity, one may suspect that there would be an increased expression of $Ca_v3.1$ in the pathological state. However, the lack of significant differences in channel expression between control and parkinsonian monkeys suggest that this may not be the case. An alternative explanation could be alteration in states of hyperpolarization in parkinsonism. It is possible that pathological dysrhythmias due to dopaminergic neurodegeneration along both the direct and indirect pathways cause afferents from the GPi/SNr to mediate increased hyperpolarization in the parkinsonian thalamus, leading to increased de-inactivation of T-type calcium channels, and thus increased instance of rebound bursting, thalamocortical dysrhythmia, and the various associated motor inhibitions associated with the disease. Further investigation in this area may yield improved understanding of the functional mechanisms of DBS and preclude more intricate and rational adjustment of stimulation parameters that exact an even better clinical outcome.

A limitation of this study is that the antibody used, though highly specific, may fail to detect all target antigens that are associated with the post synaptic density (Masugi-Tokita and Shigemoto, 2007). Since this is a common penetrance issue with synaptic immunogold localization studies, the degree to which $Ca_v3.1$ was found to be localized to symmetric and asymmetric synapses in this study should be interpreted with caution as synaptic channel

localization could conceivably be higher *in vivo*. Additionally, the density of channel expression found in both LM and EM studies may not correlate exactly with the density of the functional channel. In the brain, calcium channels undergo phosphorylation (Catterall, 2000). Specifically, phosphrylation of $Ca_v3.1$ in thalamocortical neurons has been shown to increase current amplitude (Leresche et al., 2004). Thus, with potential variances in phosphorylation states in different neuronal populations, the presence of the channel may not exactly correlate with electrophysiology and function.

Taken together, the strong dendritic and synaptic expression of thalamic $Ca_v3.1$ immunoreactivity reported in this study and the documented evidence of significant increases in T-type calcium channel mediated burst discharge in PD pathology provide solid anatomical and electrophysiological evidence for a potentially prominent role of this particular T-type channel subtype in some of the documented thalamocortical dysrhythmia seen in PD. Further studies on the spatial localization of $Ca_v3.1$ relative to other ionic channels active in thalamic bursting may be necessary to fully explain the pathological rebound bursting activity seen in parkinsonism and improve upon the current understanding of rhythmic firing in neuronal populations of the thalamus.

In recent years, researchers have recognized the potential benefits of therapies targeting calcium channels in diseases such as PD and epilepsy (Pasternak et al., 2012; Powell et al., 2014). Though dopamine replacement and deep brain stimulation have proven effective and represent the gold standard in modern PD therapy, they are associated with significant side effects, are not suitable for implementation in all patients, and do not beneficially affect the underlying pathology of the disease. With the increasing availability of selective T-type channel antagonist compounds (Li et al., 2005; Lory and Chemin, 2007; Dreyfus et al., 2010; Bladen et

al., 2015) and the emerging body of evidence detailing their therapeutic efficacy in the treatment of epilepsy (Tringham et al., 2012), insomnia (Kraus et al., 2010), and neuropathic pain (Choe et al., 2011), future studies in animal models should aim to address the specific mechanisms and potential benefits of T-type calcium channel antagonism in PD. Considering recent published studies documenting favorable safety profiles and potential neuroprotective properties of selective T-type calcium channel antagonist compounds (Kopecky et al., 2014), their potential as a much needed novel treatment to replace or be used in conjunction with dopamine replacement and stimulation therapy is an area that merits dedicated study.

V. ***Tables and Figures:***

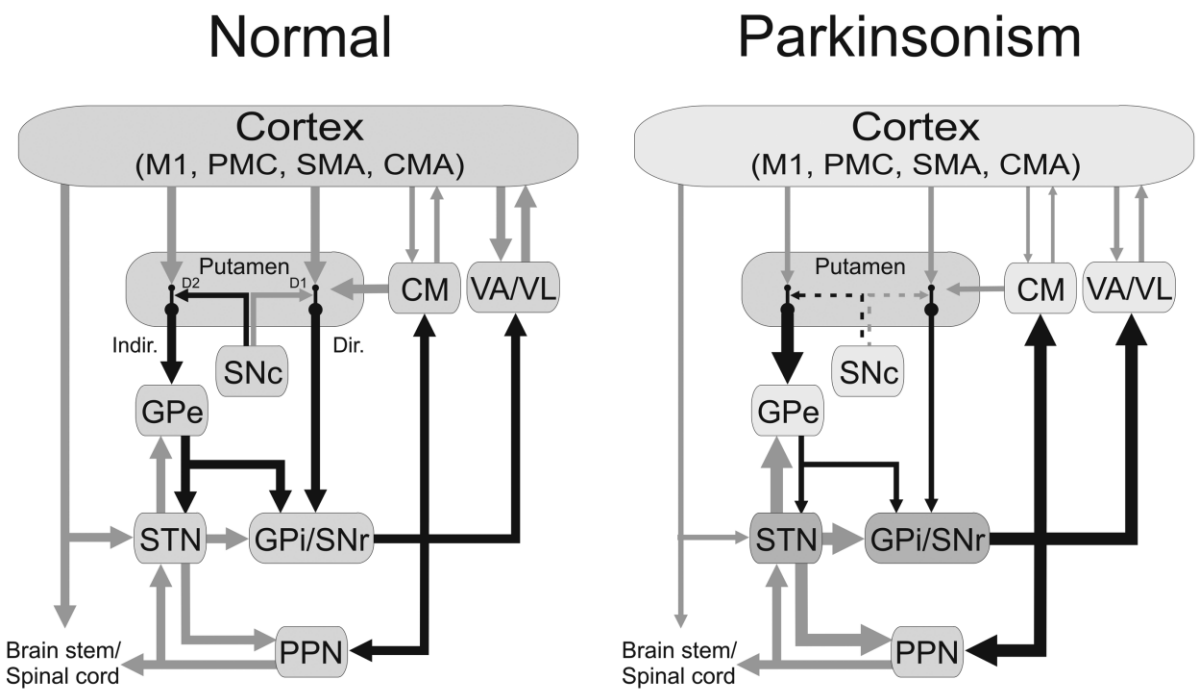

Figure 1: Impact of Parkinson's disease on neural circuitry. Black arrows indicate inhibitory connections and gray arrows indicate excitatory connections. The thickness of the arrows corresponds to their presumed activity. Abbreviations: CM – centromedian/parafascicular thalamic nuclei, CMA – cingulate motor area, Dir. – direct pathway, D1, D2 – dopamine receptor subtypes, GPe – external segment of the globus pallidus, GPi – internal segment of the globus pallidus, Indir. – indirect pathway, M1 – primary motor cortex, Pf – parafascicular nucleus of the thalamus, PMC – premotor cortex, PPN – pedunculopontine nucleus, SMA – supplementary motor area, SNc – substantia nigra pars compacta, SNr – substantia nigra pars reticulate, STN – subthalamic nucleus, VA – ventral anterior thalamic nucleus, VL – ventrolateral thalamic nucleus. Reprinted from Clinical Neurophysiology, vol. 119, no. 7, Adriana Galvan and Thomas Wichmann, "Pathophysiology of parkinsonism", pp1459-1474,

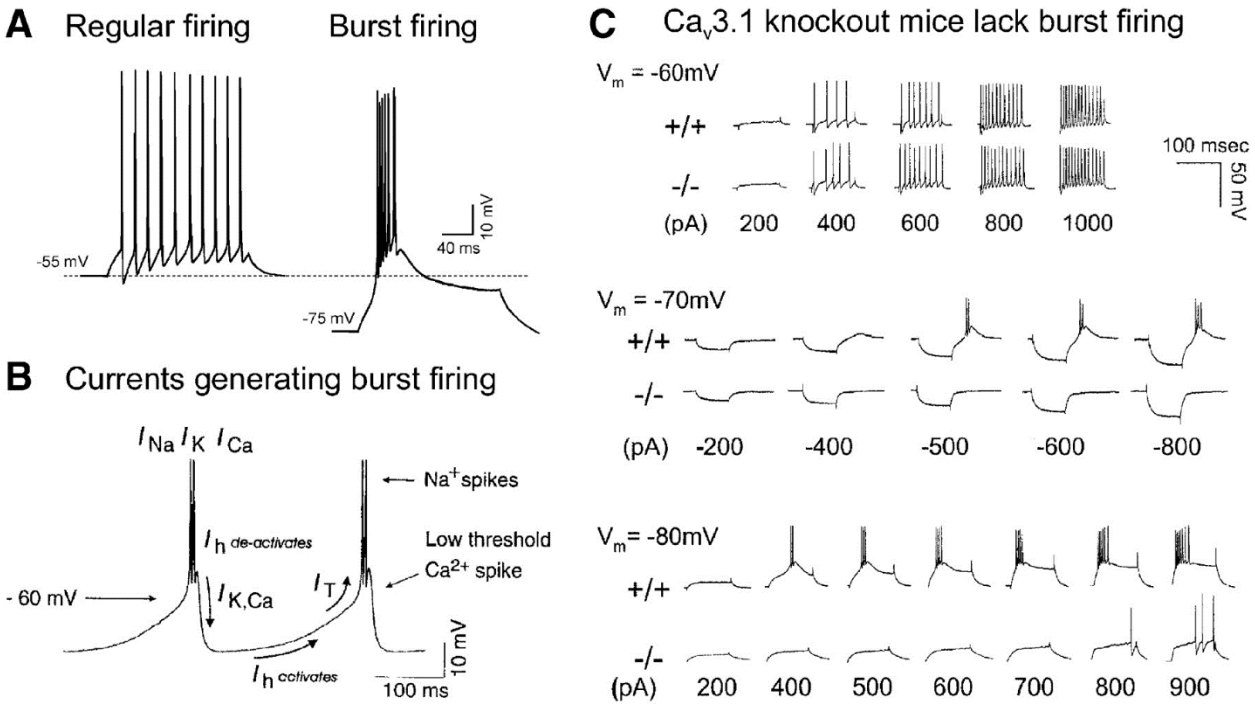

Figure 2: Low-threshold Ca^{2+} spikes generate burst firing. A: many neurons can generate two distinct patterns of action potential firing in response to a depolarizing stimulus. Regular, or tonic, firing is elicited when the neuron is depolarized from a resting membrane potential near −55 mV. In contrast, when the membrane potential is below −70 mV, the same depolarizing stimulus triggers a high-frequency burst of action potentials. (From Huguenard JR. Low-voltage-activated (T-type) calcium-channel genes identified. Trends Neurosci 21: 451–452, 1998, with permission from Elsevier Science.). B: a representative example of currents that generate burst firing. Depolarization of the plasma membrane by hyperpolarization-activated current (I_h) leads to activation of T-type currents (I_t), and a second phase of depolarization called the low-threshold Ca^{2+} spike. Riding on top of the low-threshold Ca^{2+} spike are a burst of Na^+ spikes mediated by fast voltage-gated Na^+ channels. High-threshold Ca^{2+} and K^+ currents can also be activated by the low-threshold calcium spikes. Ca^{2+} entry during the burst leads to activation of Ca^{2+}-activated K^+ currents, which in combination with voltage-gated K^+ channels repolarize the membrane. (From Bal T and McCormick DA. Synchronized oscillations in the inferior olive are controlled by the hyperpolarization-activated cation current I_h. J Neurophysiol 77: 3145–3156, 1997.) C: thalamic neurons of transgenic mice lacking expression of $Ca_v3.1$ do not fire bursts. Current-clamp recordings are from neurons held at −60, −70, or −80 mV, then depolarized or hyperpolarized by current injections of varying magnitudes as indicated below the set of traces. When the resting membrane potential is −60 mV, a depolarizing stimulus triggers tonic firing in both wild-type (+/+) and transgenic (−/−) animals. When the membrane potential (V m) is lowered to −70 mV, a hyperpolarizing stimulus triggers burst firing in neurons from wild-type, but not transgenic animals. When the resting membrane potential is −80 mV, a depolarizing stimulus only triggers burst firing in neurons from wild-type animals. (From Kim D, Song I,

Keum S, Lee T, Jeong MJ, Kim SS, McEnery MW, and Shin HS. Lack of the burst firing of thalamocortical relay neurons and resistance to absence seizures in mice lacking α1G T-type Ca^{2+} channels. Neuron 31: 35–45, 2001, with permission from Elsevier Science.). Reprinted from Physiological Reviews, vol. 83, no. 1, Edward Perez-Reyes, "Molecular Physiology of Low-Voltage-Activated T-type Calcium Channels", pp117-161, Copyright © 2003, with permission from Physiological Reviews.

Antibody	Vendor	Catalogue #	Immunogen	Immunizing Species	Dilution
$Ca_v3.1$ (monoclonal)	Neromab (Davis, CA)	73-206	Mouse aa 2052-2172	Horse	1:1000
Tyrosine Hydroxylase (monoclonal)	Merck Millipore (Darmstadt, Germany)	MAB318	Mouse aa 32-47	Horse	1:1000
vGluT2 (polyclonal)	MabTechnologies (Atlanta, GA)	VGT2-6	Human aa 560-578	Rabbit	1:5000

Table 1: Commercial sources and characteristics of primary antibodies used

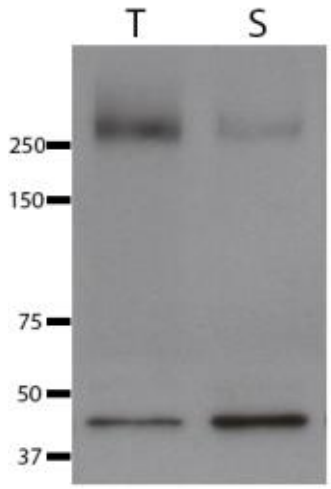

Figure 3: Western blot analysis to show the specificity of the $Ca_v3.1$ antibody when applied on monkey thalamic (T) and striatal (S) tissue. A single band corresponding to the predicted molecular weight of $Ca_v3.1$ protein (> 250 kDa) is shown in this immunoblot. Note the high level thalamic expression compared to the striatum. The band at 42kDa corresponds to actin, which was used as a reference.

	Ventrolateral (VL)	Centromedian (CM)	Parafasicular (Pf)
Control	6.24(3)	6.24(3)	6.24(3)
MPTP	6.24(3)	6.24(3)	6.24(3)

Table 2: Summary of total areas (in mm^2) and number of animals (in parentheses) used for LM densitometry assessment of $Ca_v3.1$ immunoreactivity in the VL, CM, and Pf of control and MPTP-treated monkeys

	Ventrolateral (VL)	Centromedian (CM)	Parafasicular (Pf)
Control	2214(3)	2214(3)	2214(3)
MPTP	2214(3)	2214(3)	2214(3)

Table 3: Summary of total areas (in μm^2) and number of animals (in parentheses) used for EM immunoperoxidase and immunogold localization of $Ca_v3.1$ in the VL, CM, and Pf of control and MPTP-treated monkeys. (Values are the same for immunoperoxidase and immunogold).

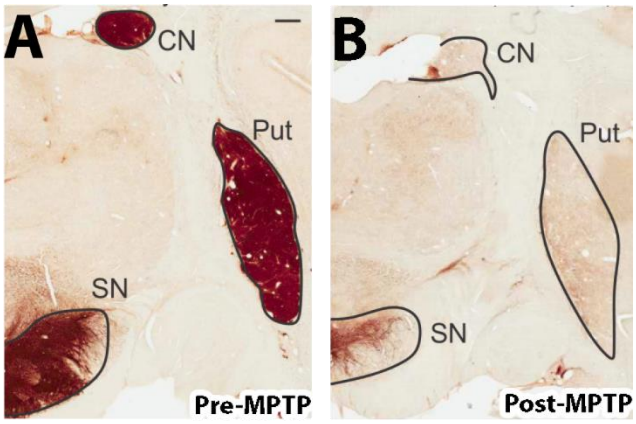

Figure 4: Example of tyrosine hydroxylase (TH) immunoperoxidase reactivity in the basal ganglia of a monkey treated with saline (A) and a monkey rendered parkinsonian by MPTP-treatment (B). Coronal sections corresponding approximately to the IA:7.95 plane in the *The Rhesus Monkey Brain in Stereotaxic Coordinates* by George Paxinos (Paxinos et al., 2000). CN: caudate nucleus; Put: putamen; SN: substantia nigra. Scale bar: 1 mm.

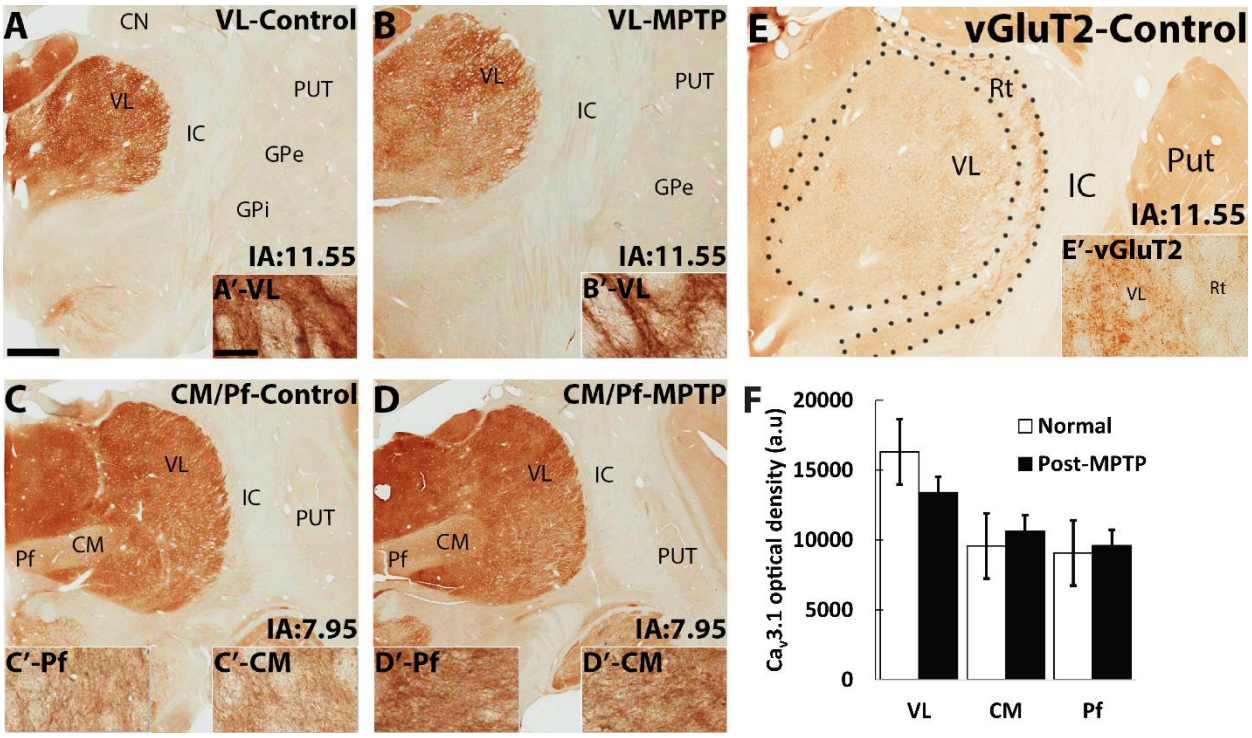

Figure 5: (A-D) Light micrographs of coronal monkey brain sections showing immunostaining for $Ca_v3.1$ at different rostrocaudal levels of control and MPTP-treated monkeys (Magnification = 0.4X). The approximate interaural coordinate for each section is indicated in the lower right of each panel. (A'-D') High-power micrographs (Magnifcation = 20X) showing $Ca_v3.1$-immunoreactivity in the VL, CM, and Pf of control and MPTP-treated animals. (E) Delineation of thalamic nuclear boundaries, based on vGluT2-immunostained coronal section of a control animal, *The Rhesus Monkey Brain in Stereotactic Coordinates* (Paxinos et al., 2000) and a coronal atlas of the macaque brain (Lanciego and Vazquez, 2012). (F) Measurements of optical intensity taken in the VL, CM and Pf (values are mean ± SEM). Significance was assessed with the Mann-Whitney Rank Sum Test and MPTP-treatment related changes were found to be insignificant at the $\alpha = 0.05$ significance level. Scale bar in A equals 2mm and applies to B, C, D, E. Scale bar in A'-VL equals 50μm and applies to B'-VL, C'-Pf, C'-CM, D'-Pf, D'-CM. Abbreviations: CM – centromedian thalamic nucleus, CN – caudate nucleus, GPe – external segment of the globus pallidus, GPi – internal segment of the globus pallidus, IC – internal capsule, Pf – parafascicular thalamic nucleus, PUT – putamen, Rt – reticular nucleus, VL – ventrolateral thalamic nucleus.

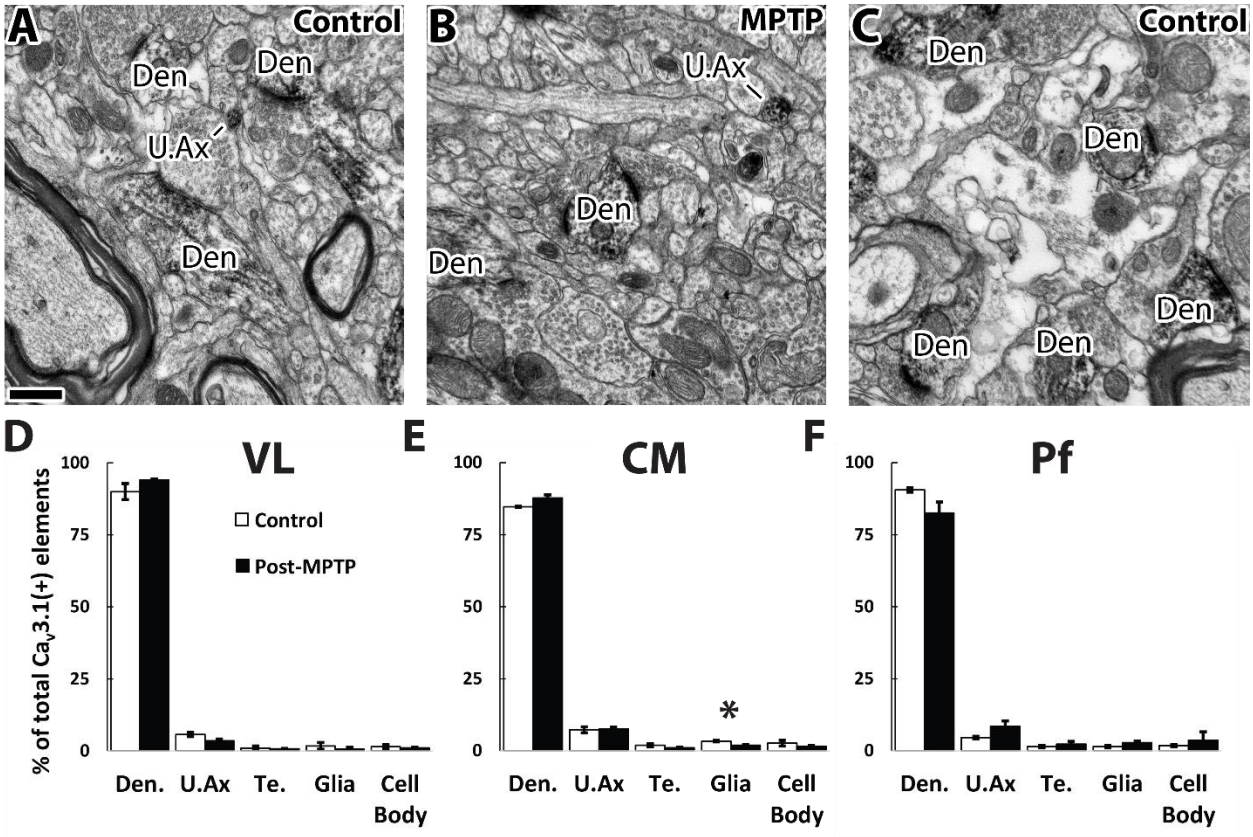

Figure 6: EM immunoperoxidase localization of $Ca_v3.1$ in the thalamus of control and MPTP-treated animals. (A-C) Representative electron micrographs of $Ca_v3.1$ immunoreactivity in thalamic nuclei of control (A, C) and MPTP-treated (B) monkeys. Immunoreactive dendritic and unmyelinated axonal processes are labeled. (D-F) Distribution of $Ca_v3.1$-immunoreactive elements in the VL, CM, and Pf of control (white) and MPTP-treated animals (black). Values are mean ± SEM and comparison between control and MPTP-treated monkeys tested with either student's t-test or Welche's t-test, depending on the variance of the groups as determined by the F-test. In E, Note a statistically significant difference (*) between treatment groups in immunoreactive glia in the CM ($p = 0.014$; t-test). Values are mean ± SEM. Abbreviations: U.Ax – unmyelinated axon, Den – dendrite. Scale bar in A= 0.5μm (applies to all micrographs).

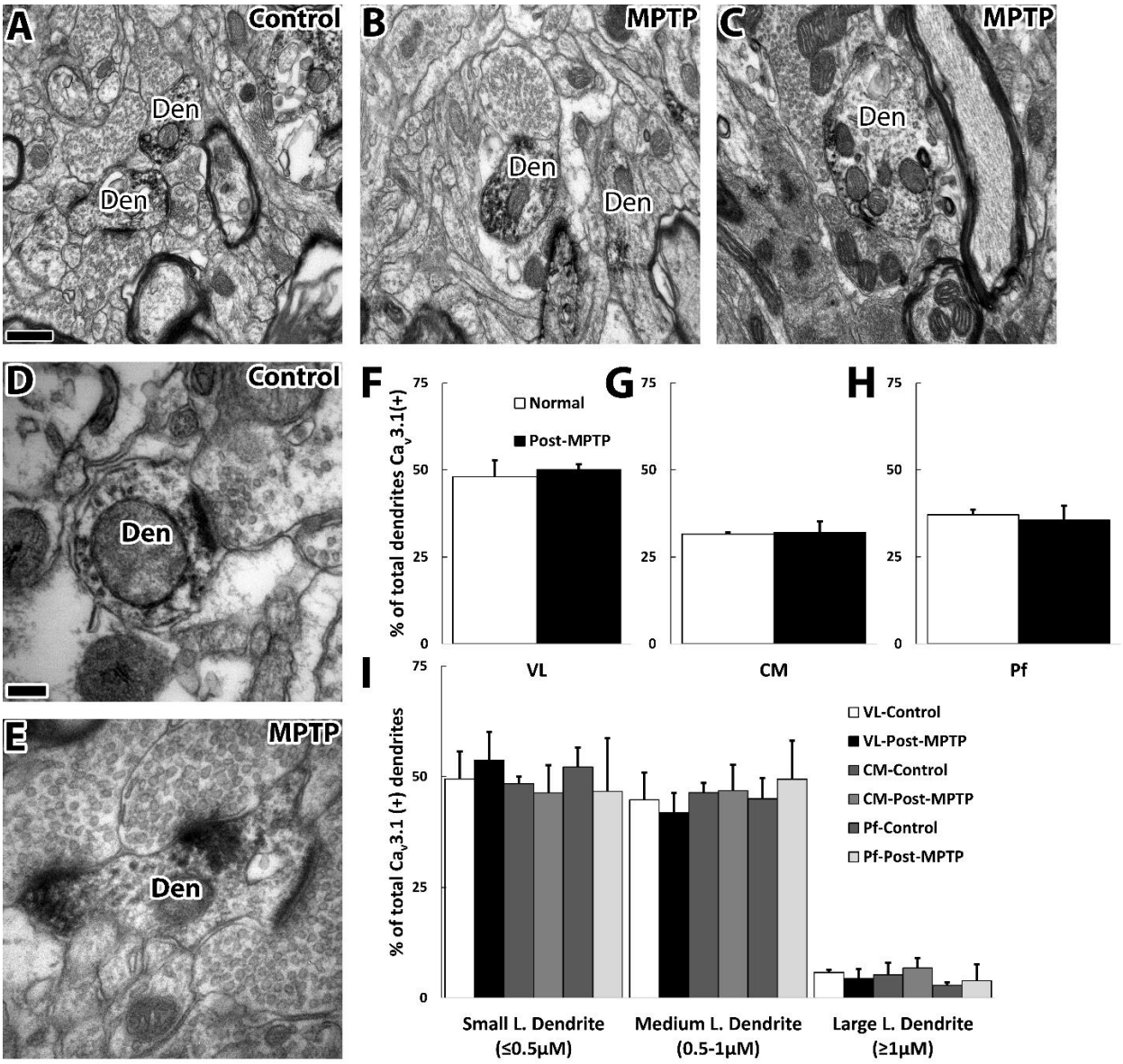

Figure 7: EM immunoperoxidase localization of $Ca_v3.1$ in thalamic dendrites of control and MPTP-treated animals. (A-C) Representative examples of $Ca_v3.1$ immunoreactivity in small (≤0.5μM), medium (0.5μM-1μM), and large (≥1μM) dendrites of thalamic nuclei of control and MPTP-treated monkeys. Note that peroxidase aggregation often occurs at the cell membrane. (D-E) High powered micrographs of dendritic $Ca_v3.1$ immunoreactivity. Note in panel E the immunoreactivity at post-synaptic specializations of putative asymmetric glutamatergic synapses. (F-G) Comparison of the percent of total dendrites labeled in the VL, CM, and Pf in control and MPTP-treated animal. No significant differences were observed between treatment conditions ($p > 0.05$; t-test). (I) Percent of total $Ca_v3.1$ immunoreactive dendrites represented by dendrites of various sizes. MPTP-treatment did not alter the distribution of $Ca_v3.1$ immunoreactivity among dendritic profiles of different sizes in the VL, CM, and Pf ($p > 0.05$; t-test). Values are mean ± SEM. Abbreviations: Den – dendrite Scale bar in A= 0.5μm (applies to B,C). Scale bar in D = 0.1μm (applies to E).

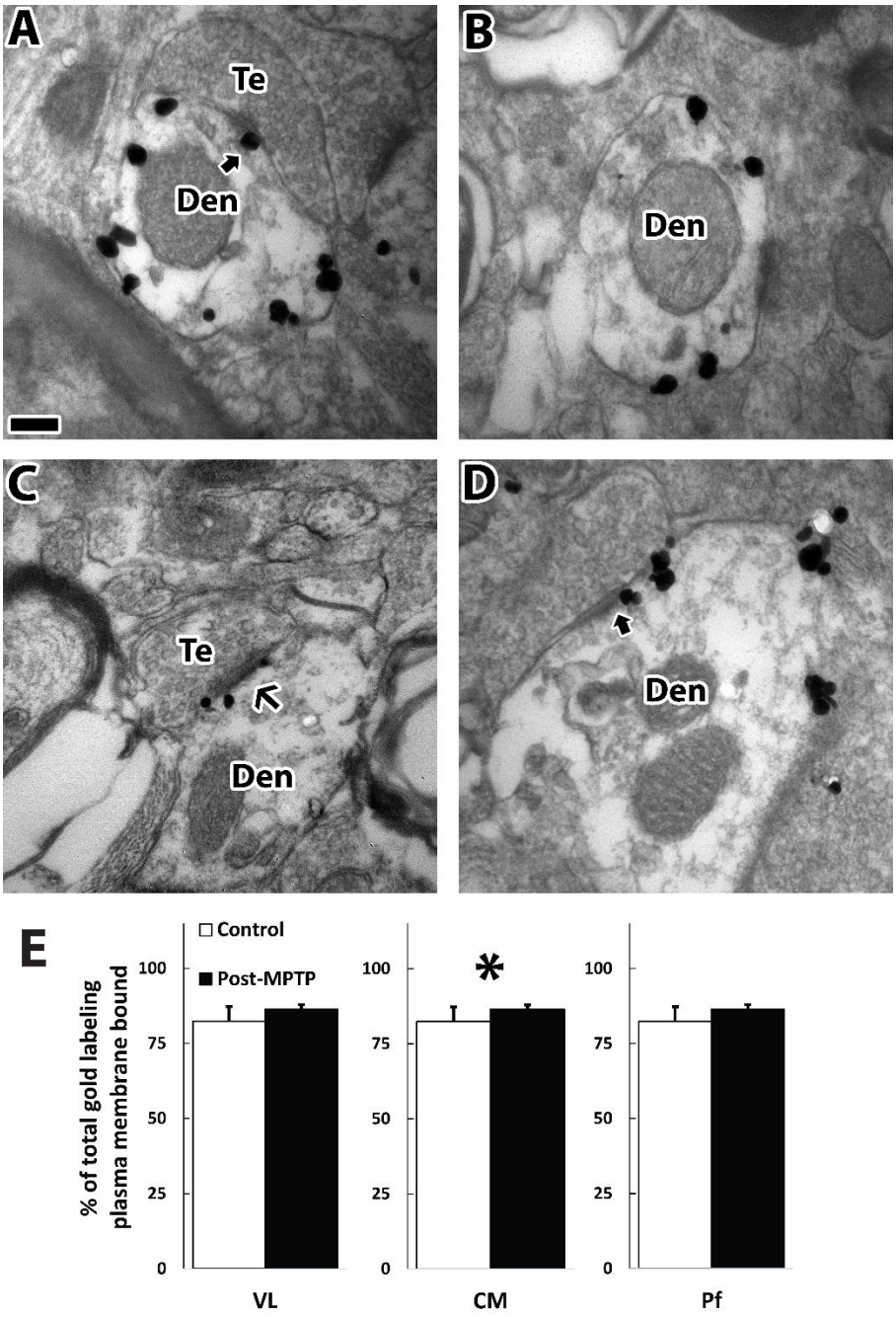

Figure 8: Pre-embedding immunogold labeling for $Ca_v3.1$ in the VL, CM, and Pf dendrites of control and MPTP-treated monkeys demonstrating subcellular localization. (A-D) Immunogold reactivity typical was found in association with the plasma membrane of dendrites, often in contact with axon terminals at symmetric (A, D, small arrows) or asymmetric (C, large arrow) synapses. Note that immunogold labeling was present at the edges of postsynaptic specializations such as densities (perisynaptic) (C, D) as well as directly apposed on both symmetric and asymmetric synapses (A, C). (E) Relative proportion of the total gold labeling in dendrites of VL, CM and Pf neurons that was plasma bound. In the VL and Pf, MPTP treatment did not

significantly affect the plasma membrane localization of the α1G subtype of T-type calcium channel. A significant increase in the percentage of membrane associated gold labeling was observed in the CM between control and MPTP-treated animals. Values are mean ± SEM. Abbreviations: Den – dendrite, Te – terminal. Scale bar in A= 0.1μm (applies to all panels).

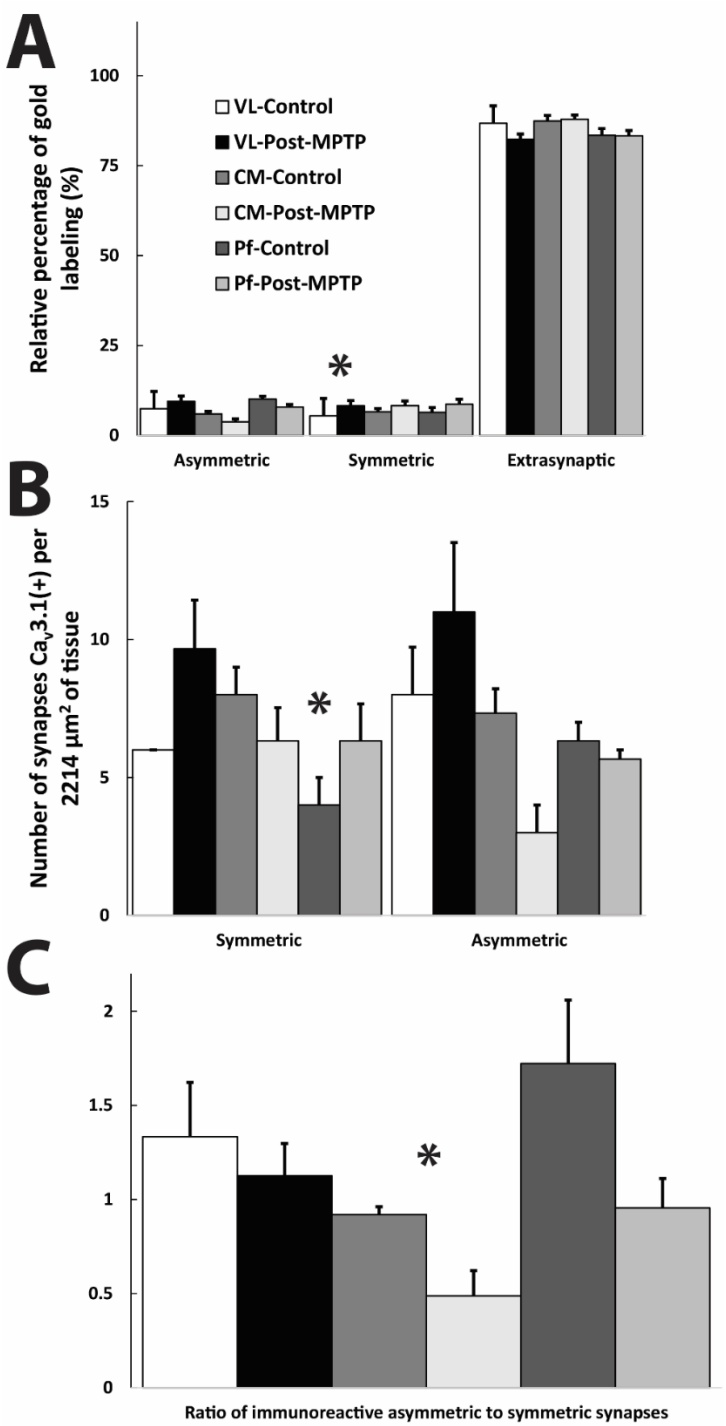

Figure 9: Pre-embedding immunogold labeling reveals the subcellular and subsynaptic localization of $Ca_v3.1$ in the VL, CM and Pf of control and MPTP-treated monkeys. (A) Immunogold reactivity in dendrites is often distributed amongst symmetric and asymmetric synapses as well extrasynaptic portions of the membrane. In the VL, MPTP-treatment led to a marginally significant difference (* in A, $p = 0.043$; t-test) in the percent of synaptic and perisynaptic membrane associated labeling found at symmetric synapses. (B) In the 2214 μm^2 of tissue analyzed per nuclei per treatment condition, the number of immunoreactive symmetric synapses varied significantly between nuclei only in the Pf of control animals (* in B, $p = 0.037$, single-factor ANOVA). MPTP-treatment had no significant effect on the number of immunoreactive symmetric and asymmetric synapses in the VL, CM, and Pf. (C) MPTP-treatment decreased the ratio of immunoreactive asymmetric to symmetric synapses with marginal significance only in the CM (*in C, $p = 0.037$, t-test). The ratio of immunoreactive asymmetric to symmetric synapses in the VL and Pf were not significantly affected by MPTP-treatment. Values are mean ± SEM.

VI. *References*:

Alvarez L, Macias R, Lopez G, Alvarez E, Pavon N, Rodriguez-Oroz MC, Juncos JL, Maragoto C, Guridi J, Litvan I, Tolosa ES, Koller W, Vitek J, DeLong MR, Obeso JA (2005) Bilateral subthalamotomy in Parkinson's disease: initial and long-term response. Brain : a journal of neurology 128:570-583.

Alvarez L, Macias R, Pavon N, Lopez G, Rodriguez-Oroz MC, Rodriguez R, Alvarez M, Pedroso I, Teijeiro J, Fernandez R, Casabona E, Salazar S, Maragoto C, Carballo M, Garcia I, Guridi J, Juncos JL, DeLong MR, Obeso JA (2009) Therapeutic efficacy of unilateral subthalamotomy in Parkinson's disease: results in 89 patients followed for up to 36 months. Journal of neurology, neurosurgery, and psychiatry 80:979-985.

Aziz TZ, Peggs D, Sambrook MA, Crossman AR (1991) Lesion of the subthalamic nucleus for the alleviation of 1-methyl-4-phenyl-1,2,3,6-tetrahydropyridine (MPTP)-induced parkinsonism in the primate. Movement disorders : official journal of the Movement Disorder Society 6:288-292.

Bal T, McCormick DA (1997) Synchronized oscillations in the inferior olive are controlled by the hyperpolarization-activated cation current I(h). Journal of neurophysiology 77:3145-3156.

Baron MS, Vitek JL, Bakay RA, Green J, Kaneoke Y, Hashimoto T, Turner RS, Woodard JL, Cole SA, McDonald WM, DeLong MR (1996) Treatment of advanced Parkinson's disease by posterior GPi pallidotomy: 1-year results of a pilot study. Annals of neurology 40:355-366.

Bergman H, Wichmann T, DeLong MR (1990) Reversal of experimental parkinsonism by lesions of the subthalamic nucleus. Science 249:1436-1438.

Bergman H, Wichmann T, Karmon B, DeLong MR (1994) The primate subthalamic nucleus. II. Neuronal activity in the MPTP model of parkinsonism. Journal of neurophysiology 72:507-520.

Bergman H, Feingold A, Nini A, Raz A, Slovin H, Abeles M, Vaadia E (1998) Physiological aspects of information processing in the basal ganglia of normal and parkinsonian primates. Trends Neurosci 21:32-38.

Bernheimer H, Birkmayer W, Hornykiewicz O, Jellinger K, Seitelberger F (1973) Brain dopamine and the syndromes of Parkinson and Huntington. Clinical, morphological and neurochemical correlations. Journal of the neurological sciences 20:415-455.

Blackstad T, Karagülle T, Ottersen O (1990) MORFOREL, a computer program for two-dimensional analysis of micrographs of biological specimens, with emphasis on immunogold preparations. Computers in biology and medicine 20:15-34.

Bladen C, McDaniel SW, Gadotti VM, Petrov RR, Berger ND, Diaz P, Zamponi GW (2015) Characterization of novel cannabinoid based T-type calcium channel blockers with analgesic effects. ACS chemical neuroscience 6:277-287.

Cain SM, Snutch TP (2013) T-type calcium channels in burst-firing, network synchrony, and epilepsy. Biochimica et Biophysica Acta (BBA) - Biomembranes 1828:1572-1578.

Catterall WA (2000) Structure and regulation of voltage-gated Ca2+ channels. Annual review of cell and developmental biology 16:521-555.

Catterall WA (2011) Voltage-gated calcium channels. Cold Spring Harbor perspectives in biology 3:a003947.

Cavelier P, Bossu JL (2003) Dendritic low-threshold Ca2+ channels in rat cerebellar Purkinje cells: possible physiological implications. Cerebellum (London, England) 2:196-205.

Choe W, Messinger RB, Leach E, Eckle VS, Obradovic A, Salajegheh R, Jevtovic-Todorovic V, Todorovic SM (2011) TTA-P2 is a potent and selective blocker of T-type calcium channels in rat sensory neurons and a novel antinociceptive agent. Molecular pharmacology 80:900-910.

Christie BR, Eliot LS, Ito K, Miyakawa H, Johnston D (1995) Different Ca2+ channels in soma and dendrites of hippocampal pyramidal neurons mediate spike-induced Ca2+ influx.

DeLong MR, Wichmann T (2007) Circuits and circuit disorders of the basal ganglia. Archives of neurology 64:20-24.

DeLong MR, Kandel E (2013) Principles of Neural Science, Fifth Edition: McGraw-Hill Education.

Destexhe A, Contreras D, Sejnowski TJ, Steriade M (1994) A model of spindle rhythmicity in the isolated thalamic reticular nucleus. Journal of neurophysiology 72:803-818.

Destexhe A, Neubig M, Ulrich D, Huguenard J (1998) Dendritic Low-Threshold Calcium Currents in Thalamic Relay Cells. The Journal of Neuroscience 18:3574-3588.

Devergnas A, Pittard D, Bliwise D, Wichmann T (2014) Relationship between oscillatory activity in the cortico-basal ganglia network and parkinsonism in MPTP-treated monkeys. Neurobiology of disease 68:156-166.

Dragicevic E, Schiemann J, Liss B (2015) Dopamine midbrain neurons in health and Parkinson's disease: Emerging roles of voltage-gated calcium channels and ATP-sensitive potassium channels. Neuroscience 284:798-814.

Dreyfus FM, Tscherter A, Errington AC, Renger JJ, Shin HS, Uebele VN, Crunelli V, Lambert RC, Leresche N (2010) Selective T-type calcium channel block in thalamic neurons reveals channel redundancy and physiological impact of I(T)window. The Journal of neuroscience : the official journal of the Society for Neuroscience 30:99-109.

Galvan A, Wichmann T (2008) Pathophysiology of parkinsonism. Clinical neurophysiology : official journal of the International Federation of Clinical Neurophysiology 119:1459-1474.

Galvan A, Hu X, Smith Y, Wichmann T (2011) Localization and pharmacological modulation of GABA-B receptors in the globus pallidus of parkinsonian monkeys. Experimental neurology 229:429-439.

Garber J, Barbee R, Bielitzki J, Clayton L, Donovan J, Hendriksen C, Kohn D, Lipman N, Locke P, Melcher J, Quimby F, Turner P, Wood G, Wurbel H (2011) Guide for the Care and Use of Laboratory Animals (8th ed.). Washington (DC): National Academies Press (US); .

Gauck V, Thomann M, Jaeger D, Borst A (2001) Spatial distribution of low- and high-voltage-activated calcium currents in neurons of the deep cerebellar nuclei. The Journal of neuroscience : the official journal of the Society for Neuroscience 21:Rc158.

Gerfen CR (1995) Dopamine Receptor Function in the Basal Ganglia. Clinical neuropharmacology 18:S162-S177.

Gonzales KK, Pare JF, Wichmann T, Smith Y (2013) GABAergic inputs from direct and indirect striatal projection neurons onto cholinergic interneurons in the primate putamen. J Comp Neurol 521:2502-2522.

Guridi J, Herrero MT, Luquin MR, Guillen J, Ruberg M, Laguna J, Vila M, Javoy-Agid F, Agid Y, Hirsch E, Obeso JA (1996) Subthalamotomy in parkinsonian monkeys. Behavioural and biochemical analysis. Brain : a journal of neurology 119 (Pt 5):1717-1727.

Hamani C, Neimat JS, Lozano AM (2007) Deep brain stimulation and chemical neuromodulation: current use and perspectives for the future. Acta neurochirurgica Supplement 97:127-133.

Hildebrand ME, Isope P, Miyazaki T, Nakaya T, Garcia E, Feltz A, Schneider T, Hescheler J, Kano M, Sakimura K, Watanabe M, Dieudonne S, Snutch TP (2009) Functional coupling between mGluR1 and Cav3.1 T-type calcium channels contributes to parallel fiber-induced fast calcium signaling within Purkinje cell dendritic spines. The Journal of neuroscience : the official journal of the Society for Neuroscience 29:9668-9682.

Hornykiewicz O (2010) A brief history of levodopa. Journal of neurology 257:S249-252.

Huguenard JR (1998) Low-voltage-activated (T-type) calcium-channel genes identified. Trends Neurosci 21:451-452.

Huguenard JR, Gutnick MJ, Prince DA (1993) Transient Ca2+ currents in neurons isolated from rat lateral habenula. Journal of neurophysiology 70:158-166.

Hutchison WD, Lozano AM, Davis KD, Saint-Cyr JA, Lang AE, Dostrovsky JO (1994) Differential neuronal activity in segments of globus pallidus in Parkinson's disease patients. Neuroreport 5:1533-1537.

Isope P, Hildebrand ME, Snutch TP (2012) Contributions of T-type voltage-gated calcium channels to postsynaptic calcium signaling within Purkinje neurons. Cerebellum (London, England) 11:651-665.

Kampa BM, Letzkus JJ, Stuart GJ (2006) Requirement of dendritic calcium spikes for induction of spike-timing-dependent synaptic plasticity. The Journal of Physiology 574:283-290.

Kavalali ET, Zhuo M, Bito H, Tsien RW (1997) Dendritic Ca2+ Channels Characterized by Recordings from Isolated Hippocampal Dendritic Segments. Neuron 18:651-663.

Khosravani H, Zamponi GW (2006) Voltage-gated calcium channels and idiopathic generalized epilepsies. Physiological reviews 86:941-966.

Kim D, Song I, Keum S, Lee T, Jeong MJ, Kim SS, McEnery MW, Shin HS (2001) Lack of the burst firing of thalamocortical relay neurons and resistance to absence seizures in mice lacking alpha(1G) T-type Ca(2+) channels. Neuron 31:35-45.

Kopecky BJ, Liang R, Bao J (2014) T-type calcium channel blockers as neuroprotective agents. Pflugers Archiv : European journal of physiology 466:757-765.

Krack P, Limousin P, Benabid AL, Pollak P Chronic stimulation of subthalamic nucleus improves levodopa-induced dyskinesias in Parkinson's disease. The Lancet 350:1676.

Kraus RL, Li Y, Gregan Y, Gotter AL, Uebele VN, Fox SV, Doran SM, Barrow JC, Yang Z-Q, Reger TS, Koblan KS, Renger JJ (2010) In Vitro Characterization of T-Type Calcium Channel Antagonist TTA-A2 and In Vivo Effects on Arousal in Mice. Journal of Pharmacology and Experimental Therapeutics 335:409-417.

Kuramoto E, Fujiyama F, Nakamura KC, Tanaka Y, Hioki H, Kaneko T (2011) Complementary distribution of glutamatergic cerebellar and GABAergic basal ganglia afferents to the rat motor thalamic nuclei. European Journal of Neuroscience 33:95-109.

Kuwajima M, Dehoff MH, Furuichi T, Worley PF, Hall RA, Smith Y (2007) Localization and expression of group I metabotropic glutamate receptors in the mouse striatum, globus pallidus, and subthalamic nucleus: regulatory effects of MPTP treatment and constitutive Homer deletion. The Journal of neuroscience : the official journal of the Society for Neuroscience 27:6249-6260.

Lanciego JL, Vazquez A (2012) The basal ganglia and thalamus of the long-tailed macaque in stereotaxic coordinates. A template atlas based on coronal, sagittal and horizontal brain sections. Brain structure & function 217:613-666.

Lee J, Kim D, Shin H-S (2004) Lack of delta waves and sleep disturbances during non-rapid eye movement sleep in mice lacking α1G-subunit of T-type calcium channels. Proceedings of the National Academy of Sciences 101:18195-18199.

Leresche N, Hering J, Lambert RC (2004) Paradoxical potentiation of neuronal T-type Ca2+ current by ATP at resting membrane potential. The Journal of neuroscience : the official journal of the Society for Neuroscience 24:5592-5602.

Li M, Hansen JB, Huang L, Keyser BM, Taylor JT (2005) Towards selective antagonists of T-type calcium channels: design, characterization and potential applications of NNC 55-0396. Cardiovascular drug reviews 23:173-196.

Limousin P, Pollak P, Benazzouz A, Hoffmann D, Le Bas JF, Broussolle E, Perret JE, Benabid AL (1995) Effect of parkinsonian signs and symptoms of bilateral subthalamic nucleus stimulation. Lancet 345:91-95.

Llinas R, Jahnsen H (1982b) Electrophysiology of mammalian thalamic neurones in vitro. Nature 297:406-408.

Lory P, Chemin J (2007) Towards the discovery of novel T-type calcium channel blockers. Expert opinion on therapeutic targets 11:717-722.

Lozano AM, Lang AE, Galvez-Jimenez N, Miyasaki J, Duff J, Hutchinson WD, Dostrovsky JO (1995) Effect of GPi pallidotomy on motor function in Parkinson's disease. Lancet 346:1383-1387.

Magnin M, Morel A, Jeanmonod D (2000) Single-unit analysis of the pallidum, thalamus and subthalamic nucleus in parkinsonian patients. Neuroscience 96:549-564.

Marchand R (1987) Histogenesis of the subthalamic nucleus. Neuroscience 21:183-195.

Markram H, Sakmann B (1994) Calcium transients in dendrites of neocortical neurons evoked by single subthreshold excitatory postsynaptic potentials via low-voltage-activated calcium channels. Proceedings of the National Academy of Sciences 91:5207-5211.

Marsden CD (1994) Problems with long-term levodopa therapy for Parkinson's disease. Clinical neuropharmacology 17 Suppl 2:S32-44.

Masugi-Tokita M, Shigemoto R (2007) High-resolution quantitative visualization of glutamate and GABA receptors at central synapses. Curr Opin Neurobiol 17:387-393.

Mathai A, Ma Y, Paré J-F, Villalba RM, Wichmann T, Smith Y (2015) Reduced cortical innervation of the subthalamic nucleus in MPTP-treated parkinsonian monkeys.

Mazloom M, Smith Y (2006) SYNAPTIC MICROCIRCUITRY OF TYROSINE HYDROXYLASE-CONTAINING NEURONS AND TERMINALS IN THE STRIATUM OF MPTP-TREATED MONKEYS. The Journal of comparative neurology 495:453-469.

Mazzone P, Stocchi F, Galati S, Insola A, Altibrandi MG, Modugno N, Tropepi D, Brusa L, Stefani A (2006) Bilateral Implantation of Centromedian-Parafascicularis Complex and GPi: A New Combination of Unconventional Targets for Deep Brain Stimulation in Severe Parkinson Disease. Neuromodulation : journal of the International Neuromodulation Society 9:221-228.

McCormick DA, Bal T (1994) Sensory gating mechanisms of the thalamus. Curr Opin Neurobiol 4:550-556.

McCormick DA, Bal T (1997) Sleep and arousal: thalamocortical mechanisms. Annual review of neuroscience 20:185-215.

McKay BE, McRory JE, Molineux ML, Hamid J, Snutch TP, Zamponi GW, Turner RW (2006) CaV3 T-type calcium channel isoforms differentially distribute to somatic and dendritic compartments in rat central neurons. European Journal of Neuroscience 24:2581-2594.

Miller WC, DeLong MR (1988) Parkinsonian symptomatology. An anatomical and physiological analysis. Annals of the New York Academy of Sciences 515:287-302.

Mitrano DA, Pare JF, Smith Y (2010) Ultrastructural relationships between cortical, thalamic, and amygdala glutamatergic inputs and group I metabotropic glutamate receptors in the rat accumbens. J Comp Neurol 518:1315-1329.

Nelson MT, Todorovic SM, Perez-Reyes E (2006) The role of T-type calcium channels in epilepsy and pain. Current pharmaceutical design 12:2189-2197.

Olanow CW, Kieburtz K, Schapira AH (2008) Why have we failed to achieve neuroprotection in Parkinson's disease? Annals of neurology 64 Suppl 2:S101-110.

Pare D, Curro'Dossi R, Steriade M (1990) Neuronal basis of the parkinsonian resting tremor: a hypothesis and its implications for treatment. Neuroscience 35:217-226.

Parent A, Hazrati LN (1995) Functional anatomy of the basal ganglia. II. The place of subthalamic nucleus and external pallidum in basal ganglia circuitry. Brain research Brain research reviews 20:128-154.

Pasternak B, Svanstrom H, Nielsen NM, Fugger L, Melbye M, Hviid A (2012) Use of calcium channel blockers and Parkinson's disease. American journal of epidemiology 175:627-635.

Paxinos G, Huang X-F, Tonga AW (1999) The Rhesus Monkey Brain in Stereotaxic Coordinates, 1st Edition: Academic Press.

Paxinos G, Huang XF, Toga AW (2000) The Rhesus Monkey Brain in Stereotaxic Coordinates: Academic Press.

Peppe A, Gasbarra A, Stefani A, Chiavalon C, Pierantozzi M, Fermi E, Stanzione P, Caltagirone C, Mazzone P (2008) Deep brain stimulation of CM/PF of thalamus could be the new elective target for tremor in advanced Parkinson's Disease? Parkinsonism & related disorders 14:501-504.

Perez-Reyes E (2003) Molecular Physiology of Low-Voltage-Activated T-type Calcium Channels.

Pessiglione M, Guehl D, Rolland AS, Francois C, Hirsch EC, Feger J, Tremblay L (2005) Thalamic neuronal activity in dopamine-depleted primates: evidence for a loss of functional segregation within basal ganglia circuits. The Journal of neuroscience : the official journal of the Society for Neuroscience 25:1523-1531.

Peters A, Palay SL, Webster HD, eds (1991) The Fine Structure of the Nervous System: Neurons and Their Supporting Cells. New York: Oxford University Press.

Powell KL, Cain SM, Snutch TP, O'Brien TJ (2014) Low threshold T-type calcium channels as targets for novel epilepsy treatments. British journal of clinical pharmacology 77:729-739.

Raju DV, Ahern TH, Shah DJ, Wright TM, Standaert DG, Hall RA, Smith Y (2008) Differential synaptic plasticity of the corticostriatal and thalamostriatal systems in an MPTP-treated monkey model of parkinsonism. European Journal of Neuroscience 27:1647-1658.

Schneider CA, Rasband WS, Eliceiri KW (2012) NIH Image to ImageJ: 25 years of image analysis. Nat Methods 9:671-675.

Smith Y, Villalba R (2008) Striatal and extrastriatal dopamine in the basal ganglia: An overview of its anatomical organization in normal and Parkinsonian brains. Movement Disorders 23:S534-S547.

Song WJ, Baba Y, Otsuka T, Murakami F (2000) Characterization of Ca(2+) channels in rat subthalamic nucleus neurons. Journal of neurophysiology 84:2630-2637.

Steriade M (2005) Sleep, epilepsy and thalamic reticular inhibitory neurons. Trends Neurosci 28:317-324.

Su PC, Tseng HM, Liu HM, Yen RF, Liou HH (2002) Subthalamotomy for advanced Parkinson disease. Journal of neurosurgery 97:598-606.

Tai CH, Yang YC, Pan MK, Huang CS, Kuo CC (2011) Modulation of subthalamic T-type Ca(2+) channels remedies locomotor deficits in a rat model of Parkinson disease. The Journal of clinical investigation 121:3289-3305.

Tai CH, Pan MK, Lin JJ, Huang CS, Yang YC, Kuo CC (2012) Subthalamic discharges as a causal determinant of parkinsonian motor deficits. Annals of neurology 72:464-476.

Talley EM, Cribbs LL, Lee JH, Daud A, Perez-Reyes E, Bayliss DA (1999) Differential distribution of three members of a gene family encoding low voltage-activated (T-type) calcium channels. The Journal of neuroscience : the official journal of the Society for Neuroscience 19:1895-1911.

Timmermann L, Gross J, Dirks M, Volkmann J, Freund HJ, Schnitzler A (2003) The cerebral oscillatory network of parkinsonian resting tremor. Brain : a journal of neurology 126:199-212.

Tringham E, Powell KL, Cain SM, Kuplast K, Mezeyova J, Weerapura M, Eduljee C, Jiang X, Smith P, Morrison J-L, Jones NC, Braine E, Rind G, Fee-Maki M, Parker D, Pajouhesh H, Parmar M, O'Brien TJ, Snutch TP (2012) T-Type Calcium Channel Blockers That Attenuate Thalamic Burst Firing and Suppress Absence Seizures. Science Translational Medicine 4:121ra119-121ra119.

Vila M, Perier C, Feger J, Yelnik J, Faucheux B, Ruberg M, Raisman-Vozari R, Agid Y, Hirsch EC (2000) Evolution of changes in neuronal activity in the subthalamic nucleus of rats with unilateral lesion of the substantia nigra assessed by metabolic and electrophysiological measurements. The European journal of neuroscience 12:337-344.

Villalba RM, Lee H, Smith Y (2009) Dopaminergic Denervation and Spine Loss in the Striatum of MPTP-treated Monkeys. Experimental neurology 215:220-227.

Villalba RM, Raju DV, Hall RA, Smith Y (2006) GABAB receptors in the centromedian/parafascicular thalamic nuclear complex: An ultrastructural analysis of GABABR1 and GABABR2 in the monkey thalamus. Journal of Comparative Neurology 496:269-287.

Wichmann T, DeLong MR (1996) Functional and pathophysiological models of the basal ganglia. Current Opinion in Neurobiology 6:751-758.

Yang YC, Tai CH, Pan MK, Kuo CC (2014) The T-type calcium channel as a new therapeutic target for Parkinson's disease. Pflugers Archiv : European journal of physiology 466:747-755.

Yunker AMR, Sharp AH, Sundarraj S, Ranganathan V, Copeland TD, McEnery MW (2003) Immunological characterization of T-type voltage-dependent calcium channel CaV3.1 (alpha1G) and CaV3.3 (alpha1I) isoforms reveal differences in their localization, expression, and neural development. Neuroscience 117:321-335.

Zhang Y, Jiang X, Snutch TP, Tao J (2013) Modulation of low-voltage-activated T-type Ca2 + channels. Biochimica et Biophysica Acta - Biomembranes 1828:1550-1559.

Zhou Q, Godwin DW, O'Malley DM, Adams PR (1997) Visualization of calcium influx through channels that shape the burst and tonic firing modes of thalamic relay cells. Journal of neurophysiology 77:2816-2825.